David Taylor Research Center

Bethesda, MD 20084–5000

DTRC-89/023   September 1989

Ship Hydromechanics Department
Research and Development Report

A Vane-Wheel Propulsor for a Naval Auxiliary

by
Benjamin Y.-H. Chen
Arthur M. Reed
Ki-Han Kim

89 10 19 064

MAJOR DTRC TECHNICAL COMPONENTS

CODE 011 DIRECTOR OF TECHNOLOGY, PLANS AND ASSESSMENT

12 SHIP SYSTEMS INTEGRATION DEPARTMENT

14 SHIP ELECTROMAGNETIC SIGNATURES DEPARTMENT

15 SHIP HYDROMECHANICS DEPARTMENT

16 AVIATION DEPARTMENT

17 SHIP STRUCTURES AND PROTECTION DEPARTMENT

18 COMPUTATION, MATHEMATICS & LOGISTICS DEPARTMENT

19 SHIP ACOUSTICS DEPARTMENT

27 PROPULSION AND AUXILIARY SYSTEMS DEPARTMENT

28 SHIP MATERIALS ENGINEERING DEPARTMENT

DTRC ISSUES THREE TYPES OF REPORTS:

1. **DTRC reports, a formal series,** contain information of permanent technical value. They carry a consecutive numerical identification regardless of their classification or the originating department.

2. **Departmental reports, a semiformal series,** contain information of a preliminary, temporary, or proprietary nature or of limited interest or significance. They carry a departmental alphanumerical identification.

3. **Technical memoranda, an informal series,** contain technical documentation of limited use and interest. They are primarily working papers intended for internal use. They carry an identifying number which indicates their type and the numerical code of the originating department. Any distribution outside DTRC must be approved by the head of the originating department on a case-by-case basis

REPORT DOCUMENTATION PAGE	Form Approved OMB No 0704 0188

1a REPORT SECURITY CLASSIFICATION UNCLASSIFIED	1b RESTRICTIVE MARKINGS

2a SECURITY CLASSIFICATION AUTHORITY	3 DISTRIBUTION AVAILABILITY OF REPORT
2b DECLASSIFICATION/DOWNGRADING SCHEDULE	APPROVED FOR PUBLIC RELEASE; DISTRIBUTION IS UNLIMITED.

4 PERFORMING ORGANIZATION REPORT NUMBER(S) DTRC-89/023	5 MONITORING ORGANIZATION REPORT NUMBERS

6a NAME OF PERFORMING ORGANIZATION Ship Hydromechanics Department David Taylor Research Center	6b OFFICE SYMBOL (If applicable) Code 1544	7a NAME OF MONITORING ORGANIZATION
6c. ADDRESS (City, State, and ZIP Code) Bethesda, MD 20084-5000		7b ADDRESS (City, State, and ZIP Code)

8a NAME OF FUNDING/SPONSORING ORGANIZATION Office of Naval Technology	8b OFFICE SYMBOL (If applicable) Code 21	9 PROCUREMENT INSTRUMENT IDENTIFICATION NUMBER

8c. ADDRESS (City, State, and ZIP Code) 800 N. Quincy St. Arlington, VA 22217	10 SOURCE OF FUNDING NUMBERS			
	PROGRAM ELEMENT NO	PROJECT NO	TASK NO	WORK UNIT ACCESSION NO
	62121N	4B401AD	RH21E40	

11 TITLE (Include Security Classification)

A VANE-WHEEL PROPULSOR FOR A NAVAL AUXILIARY

12 PERSONAL AUTHOR(S)
Chen, Benjamin Y.-H., Reed, Arthur M., and Kim, Ki-Han

13a TYPE OF REPORT Final	13b TIME COVERED FROM _____ TO _____	14 DATE OF REPORT (Year, Month, Day) 1989 September	15 PAGE COUNT 37

16 SUPPLEMENTARY NOTATION
Main text was presented at the Symposium on Hydrodynamic Performance Enhancement for Marine Applications, Newport, Rhode Island, 31 October--1 November 1988

17	COSATI CODES		18 SUBJECT TERMS (Continue on reverse if necessary and identify by block number)
FIELD	GROUP	SUB-GROUP	Vane-Wheel Propulsors, Interaction Velocities, Mass Conservation, Momentum Conservation, Circulation Conservation

19 ABSTRACT (Continue on reverse if necessary and identify by block number)

A design methodology for vane-wheel propulsors has been developed using three fundamental principles. Momentum conservation requires the net force generated by the vane-wheel propulsor to be balanced by the barebody drag and the drag due to propeller and hull interactions. Mass conservation determines the distribution of the vane-wheel circulation once the rotor circulation distribution is specified. Circulation conservation determines the magnitude of the circulation distribution to ensure zero torque on the vane wheel. A vane-wheel propulsor has been designed for uniform flow at the operating point of the propulsor on the naval auxiliary AO-177 JUMBO. Model-scale experimental results showed that the performance predictions agree well with the measurements. The shaft horsepower with vane wheel is 9 percent lower than without.

20 DISTRIBUTION/AVAILABILITY OF ABSTRACT [X] UNCLASSIFIED/UNLIMITED ☐ SAME AS RPT ☐ DTIC USERS	21 ABSTRACT SECURITY CLASSIFICATION UNCLASSIFIED
22a NAME OF RESPONSIBLE INDIVIDUAL Benjamin Y.-H. Chen	22b TELEPHONE (Include Area Code) (202) 227-1450 · 22c OFFICE SYMBOL Code 1544

DD Form 1473, JUN 86   Previous editions are obsolete   SECURITY CLASSIFICATION OF THIS PAGE

S/N 0102-LF-014-6603

UNCLASSIFIED

CONTENTS

FIGURES

FIGURES (Continued)

TABLES

NOMENCLATURE

K	Blade number
m	Control point
M	Number of control points
q	Torque ratio, $q = Q_2/Q_1$
Q	Torque
T	Thrust
u_a	Axial induced velocity
u_r	Radial induced velocity
u_t	Tangential induced velocity
u_{aii}	Axial self-induced velocity for the ith component
u_{aij}	Axial velocity induced by the jth component on the ith component
u_{tii}	Tangential self-induced velocity for the ith component
u_{tij}	Tangential velocity induced by the jth component on the ith component
V_a	Axial inflow velocity
V_t	Tangential inflow velocity
$w_c(X_R)$	Circumferential mean wake fraction
w_T	Propeller effective wake fraction
w_v	Volumetric mean wake fraction
$w_x(X_R)$	Local wake fraction
X_R	Nondimensional radius measured from the shaft axis
ω	Angular velocity
λ	Lagrange multiplier
Γ	Circulation

A-1

v

ϱ Fluid density

Subscripts:

$i = 1, 2$

$j = 1, 2$

1 − Rotor

2 − Vane wheel

      All other notation in this report is in accordance with the International Towing Tank Conference (ITTC) Standard Symbols.*

---

*"International Towing Tank Conference Standard Symbol 1976" The British Ship Research Association, BSRA Technical Memorandum No. 500 (May 1976).

ABSTRACT

*A design methodology for vane-wheel propulsors has
been developed using three fundamental principles.
Momentum conservation requires the net force generated by
the vane-wheel propulsor to be balanced by the barebody
drag and the drag due to propeller and hull interactions.
Mass conservation determines the distribution of the vane-
wheel circulation once the rotor circulation distribution is
specified. Circulation conservation determines the magnitude
of the circulation distribution to ensure zero torque on the
vane wheel. A vane-wheel propulsor has been designed for
uniform flow at the operating point of the propulsor on the
naval auxiliary AO-177 JUMBO. Model-scale experimental
results showed that the performance predictions agree well
with the measurements. The shaft horsepower with vane
wheel is 9 percent lower than without.*

INTRODUCTION

In 1966, Professor Otto Grim [1] proposed the idea of placing a freely
rotating device (not mechanically driven) behind a conventional propeller as an
energy saving device for highly loaded propulsors. This concept, called a vane-
wheel propulsor, works by reclaiming part of the energy normally lost in the
propeller slip stream and converting the energy into additional thrust. The rotor
in a vane-wheel propulsor performs in the manner of a conventional propeller,
whereas the vane wheel has an inner part which acts as a turbine and an outer
part which acts as a propeller producing thrust. The overall diameter of the
vane wheel is larger than the rotor.

Initially, the concept of the vane-wheel propulsor was slow to catch on with
naval architects and ship owners. However, in the last decade, the vane-wheel
propulsor has been applied to a number of ships, particularly to tankers and
bulk carriers. The latest and perhaps the most infamous application of a vane-
wheel propulsor is in the repropulsion of the cruise ship QE2.

We have called the QE2 vane-wheel application infamous because five of
the seven vane-wheel blades failed during trials. The failure is believed to be due
to inappropriate design thickness near the root. This results in an inability of
the vane-wheel blades to unsteady forces during maneuvers. Even though, the
QE2 has significantly lower thrust loading than seen on large tanker and bulk
carrier forms, and extends the proposed operational speeds to much higher levels
than have been reported to date. Thus, it seemed appropriate to evaluate the
technology of vane-wheel propulsors on naval auxiliaries.

The improvements of the propulsive efficiency of the vane wheel propulsor
are due to the following reasons.

(1) Reduced rotational energy losses in the propeller slipstream.

(2) Reduced axial kinetic energy losses in the propeller slipstream.

(3) Production of additional thrust.

The first item comes about because the turbine part of the vane-wheel propulsor
induces tangential velocity opposite to the rotor induced tangential velocity at

1

the vane-wheel plane. The second source of improvement results from the fact that the vane wheel causes the maximum blade loading to shift inboard. As mentioned previously, the final point results from the operation of the outer portion of the vane wheel.

In 1980, Grim [2] discussed the vane-wheel propulsor concept in the Second Georg Weinblum Memorial Lecture. He described a series of experiments performed at the Hamburg Ship Model Tank on: a conventional propeller, a contrarotating propeller, a propeller with fixed guide mechanism, and a vane-wheel propulsor. These experiments showed that the propeller with guide mechanism was 5.32 percent more efficient than the conventional propeller and the propeller with vane wheel is 4.38 to 9.19 percent more efficient depending on the vane-wheel diameter.

Kehr [3] showed that the velocities induced by the propeller on the vane wheel are of great importance in the vane-wheel propulsor design. He gave a preliminary design methodology for vane-wheel propulsors which employed lifting-line theory, and included the mutual interaction velocities between the propeller and the vane wheel. However, a detailed design was not provided.

Blaurock [4] presented model tests of a vane-wheel propulsor in combination with a fixed pitch (FP) propeller and a controllable pitch (CP) propeller. These experiments showed that the efficiency can increase up to 5 percent depending on the specific thrust loading coefficient of the propeller. Efficiency gains of around 10 percent were typical depending on the specific loading conditions of the propeller and the type of the ship concerned.

Van Beek and Lips [5] presented the repropulsion of the cruise ship QE-2 using two CP propellers with a vane wheel. They showed that the efficiency increases by 3.6 percent and that only moderate cavitation occurs despite the high ship speed.

In the present study, a design methodology for vane-wheel propulsors was developed using the principles of momentum, mass, and circulation conservation. The mutual interaction velocities between the rotor and the vane wheel were predicted using the lifting-line theory. A vane-wheel propulsor was designed for uniform flow at the loading condition of the naval auxiliary AO-177 JUMBO. Model data for the vane-wheel propulsor in uniform flow have been measured.

DESIGN METHODOLOGY FOR VANE-WHEEL PROPULSORS

Vane-wheel propulsor designs need to satisfy three fundamental principles; momentum, mass, and circulation conservation. Momentum conservation requires that the net force generated by the vane-wheel propulsor be balanced by the barebody drag and the drag due to the hull-propulsor interactions. The interaction term, thrust deduction, is caused by the acceleration of the flow as it approaches the propeller, and results in a pressure reduction which generates additional drag on the hull. Since the thrust deduction factor for a vane-wheel propulsor is unknown, the thrust deduction for a single-screw propeller is employed in the present design methodology.

Mass conservation determines the distribution of the vane-wheel circulation once the rotor circulation is specified. In other words, the turbine part of the vane-wheel propulsor is determined by imparting the same mass flow as the rotor. Based on the mass conservation, the nondimensional radius of the turbine part of the vane-wheel propulsor, R_T, must be chosen so that the following relation holds

2

$$R_R^2 \int_{X_{RRhub}}^1 (V_{aR} + u_{aRR} + u_{aRT}) X_{RR} dX_{RR}$$

$$= R_T^2 \int_{X_{RThub}}^1 (V_{aT} + u_{aTT} + u_{aTR}) X_{RT} dX_{RT} \tag{1}$$

where V_{aR} and V_{aT} are the axial inflows for the rotor and the turbine part of the vane wheel, u_{aRR} and u_{aTT} are the axial self-induced velocities of the rotor and turbine, u_{aRT} and u_{aTR} are the axial velocity induced by the turbine on the rotor and the rotor on the turbine, X_{RR} and X_{RT} are the local radii of the rotor and turbine, X_{RRhub} and X_{RThub} are the radii of the rotor and turbine at the hub nondimensionalized on the radius of the rotor R_R. The nondimensional radius of the turbine part of the vane wheel needs to be calculated through an iterative process until it is equal to the wake contraction ratio of the rotor in the presence of the vane wheel.

Circulation conservation determines the magnitude of the vane-wheel circulation distribution to ensure zero torque on the vane wheel.

A flow chart of the design methodology is shown in Fig. 1. Traditionally, for a single-screw propeller, the effects of the hull on the flow and of the hull-propulsor interactions are represented by the nominal wake and the hull-propulsor interaction coefficients. Because of the differences in blade numbers and rotational speeds between the rotor and the vane wheel, the real flow passing through these two devices is an unsteady flow both in space and time, Nonetheless, the circumferential averaged flow is employed in the calculations to simplify the design procedure. Since a wake survey only provides the nominal wake, the effect of the presence of a propulsor on the wake should be calculated. This can be achieved by employing either the traditional naval architectural procedure or by a method based on inviscid axisymmetric flow theory (Huang and Groves [6]). The traditional naval architectural procedure determines the effective wake as

$$(1 - w_x(x_R)) = \frac{1 - w_T}{1 - w_v} (1 - w_c(x_R)) \tag{2}$$

where $(1 - w_c(x_R))$ is the nondimensional circumferential mean axial velocity component (nominal wake) from the wake survey, $1 - w_T$ is the Taylor wake and $1 - w_v$ the volumetric mean nominal wake.

In the preliminary design stage, lifting-line theory plays an important role due to the following reasons. First, the lifting line provides the radial distribution of circulation and the resulting thrust and torque (normally, these come from a Trefftz plane analysis). Second, lifting-line theory economically provides an optimum design from efficiency, strength, and cavitation considerations through a large number of parametric studies. Because the large number of parameters and mutual interactions need to be calculated between the
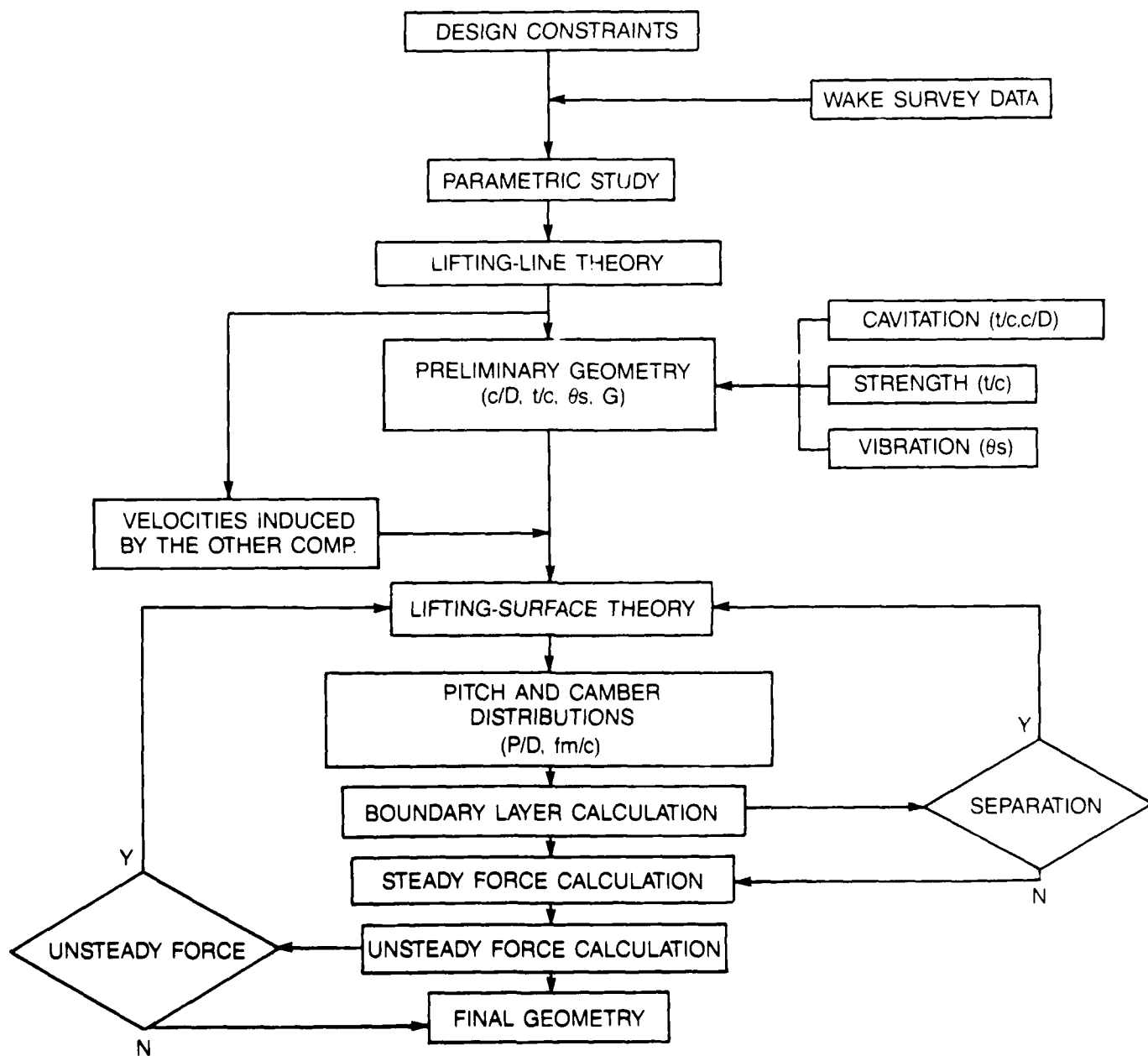
3

Fig. 1. A flow chart of the vane-wheel propulsor design methodology.

4

rotor and the vane wheel, this economy is particularly important for compound propulsors such as the vane-wheel propulsor.

Traditionally, the lifting-line analysis of a compound propulsor is carried out by coupling single-screw propeller codes in an iterative process. For the present study, a lifting-line theory developed by Kerwin et. al [7] which can solve the multi-component propulsor design problem directly was employed. In addition, their theory computes the induced velocities, not only the self-induced velocities of each component, but also the velocities induced by the components on each other. Fig. 2 shows the velocity diagrams for a vane-wheel propulsor including the self-induced velocity and the mutual interaction velocity.

Based on the thrust identity, Kerwin et. al utilizes a variational approach to optimize the circulation. In other words, for a prescribed total thrust, T, and a prescribed torque ratio, q, between the two components, the optimum circulation of each component can be obtained by minimizing the total power. A description of the variational approach is as follows.

Component 1 represents rotor and component 2 represents vane wheel.

Minimize: $\omega_1 Q_1 + \omega_2 Q_2$

Subject to the constraints: $T_1 + T_2 - T = 0$ (3)

and $Q_2 - qQ_1 = 0$ (4)

a constrained objective function is formed:

$$H = \omega_1 Q_1 + \omega_2 Q_2 + \lambda_1 (T_1 + T_2 - T) + \lambda_2 (Q_2 - qQ_1)$$ (5)

where ω_1 and ω_2 are the angular velocities for each component, λ_1 and λ_2 are Lagrange multipliers, T_1 and T_2 are the thrusts for each component, and Q_1 and Q_2 are the torques for each component. Thrusts and torques are computed using the following formulas:

$$T_i = \varrho \sum_{m=1}^{M_i} K_i \Gamma_{im} \Delta X_{Rim} (V_{tim} + \omega_i X_{Rim} + u_{tim}) \quad (i = 1,2),$$ (6)

and

$$Q_i = \varrho \sum_{m=1}^{M_i} K_i \Gamma_{im} \Delta X_{Rim} X_{Rim} (V_{aim} + u_{aim}) \quad (i = 1,2),$$ (7)

where X_{Rim} is the local radius from the shaft axis to the control point m, ΔX_{Rim} is the radial distance between the two lattice points surrounding control points m, K_i is the number of blades and M_i the number of control points. Γ_{im} is the circulation, V_{aim} and V_{tim} are the axial and the tangential inflow velocities, and u_{aim} and u_{tim} are axial and tangential induced velocities at the control points. These induced velocities include the self-induced velocities and the velocities induced by the other component. The velocities u_{aim} and u_{tim} can be expressed as follows.

5

$u_{tRT} \approx 0$

u_{aRR}

u_{tRR}

u_{aRT}

$\varepsilon_R \dfrac{dL_R}{dr}$

$\dfrac{dL_R}{dr}$

$\dfrac{dT_R}{dr}$

$V_x(r)\,(1-w_R)$

$\dfrac{1}{r}\dfrac{dQ_R}{dr}$

$\Gamma_R(r)$

$\omega_R r$

$V_t(r)$

β β_i

ROTOR

$V_t(r)$ $\omega_T r$

u_{tTR}

u_{aTT} u_{tTT}

u_{aTR}

$V_x(r)\,(1-w_T)$

β

β_i

$\Gamma_T(r)$

$\dfrac{1}{r}\dfrac{dQ_T}{dr}$

$\dfrac{dL_T}{dr}$

$\dfrac{dT_T}{dr}$

$\varepsilon_T \dfrac{dL_T}{dr}$

TURBINE

u_{aPP}

u_{tPP}

$\varepsilon_p \dfrac{dL_P}{dr}$

$\dfrac{dL_P}{dr}$

$\dfrac{dT_P}{dr}$

$V_x(r)\,(1-w_P)$

$\dfrac{1}{r}\dfrac{dQ_P}{dr}$

$\Gamma_P(r)$

$\omega_P r$

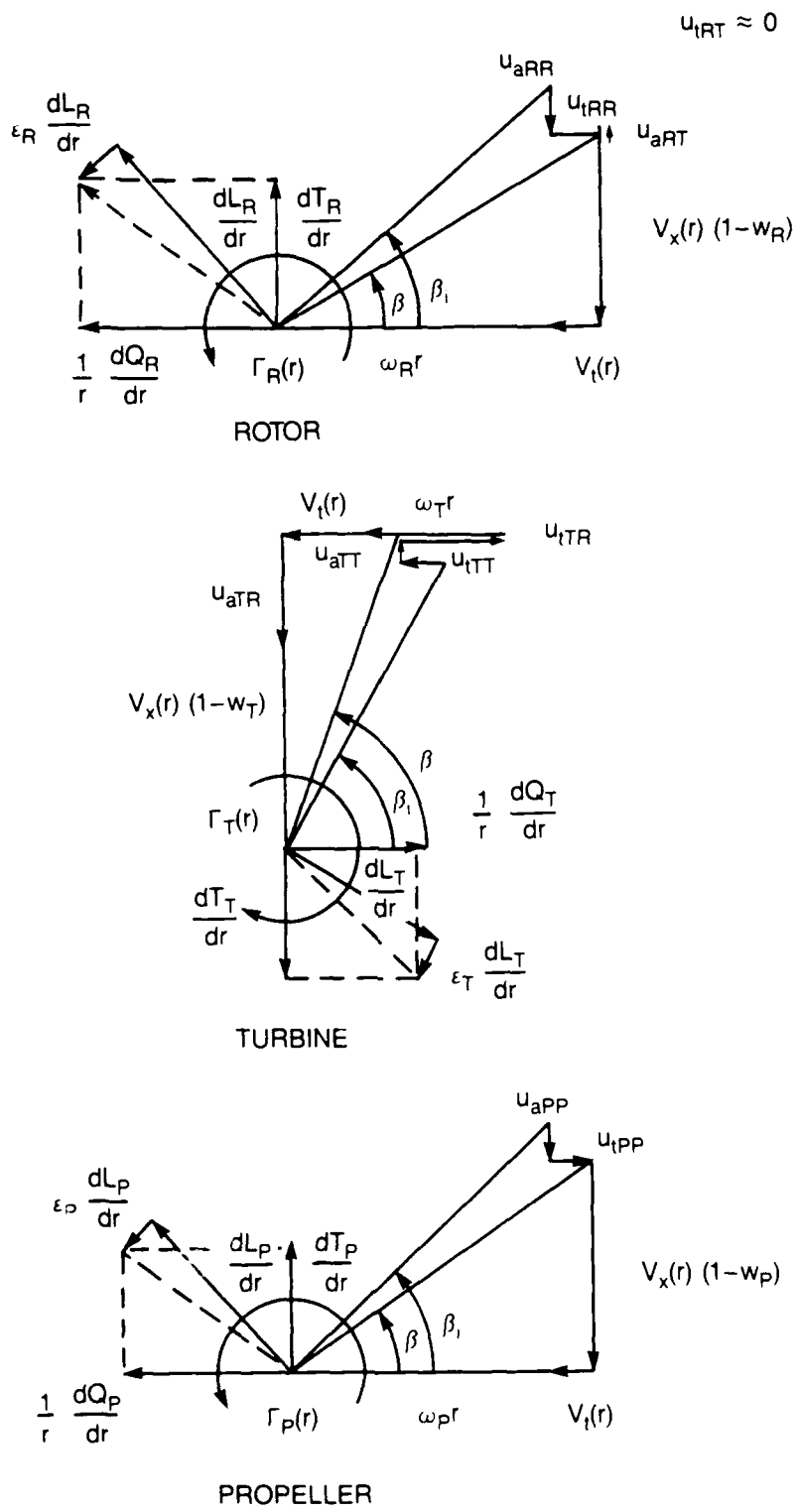$V_t(r)$

β β_i

PROPELLER

Fig. 2. Velocity diagram for a vane-wheel propulsor.

6

$$u_{a1m} = \sum_{n=1}^{M_1} \Gamma_{1n} u_{a1m,1n} + \sum_{n=1}^{M_2} \Gamma_{2n} u_{a1m,2n}, \tag{8}$$

$$u_{a2m} = \sum_{n=1}^{M_1} \Gamma_{1n} u_{a2m,1n} + \sum_{n=1}^{M_2} \Gamma_{2n} u_{a2m,2n}, \tag{9}$$

$$u_{t1m} = \sum_{n=1}^{M_1} \Gamma_{1n} u_{t1m,1n} + \sum_{n=1}^{M_2} \Gamma_{2n} u_{t1m,2n}, \tag{10}$$

and

$$u_{t2m} = \sum_{n=1}^{M_1} \Gamma_{1n} u_{t2m,1n} + \sum_{n=1}^{M_2} \Gamma_{2n} u_{t2m,2n}, \tag{11}$$

The constrained objective function H is expanded from Eqs. (5), (8), (9), (10), and (11) and its partial derivatives with respect to the unknown circulations and Lagrange multipliers are set equal to zero. This process provides $M_1 + M_2 + 2$ equations which can be solved for the circulations at the control points and the Lagrange multipliers λ_1 and λ_2. Hence, one obtains

$$\frac{\partial H}{\partial \Gamma_i} = 0 \quad (= 1,...,\ M_i,\ i = 1,2), \tag{12}$$

and

$$\frac{\partial H}{\partial \lambda_i} = 0, \quad (i = 1,2). \tag{13}$$

As mentioned before, one of the most important tasks in the vane-wheel propulsor design is that of calculating the induced velocities. Chen and Reed [8] show that the use of interaction velocities calculated by the lifting-line theory is sufficient for use in design when the propeller loadings are moderate and the two components are not too close to each other. Since the rotor loading in the present case is a moderate one, the induced velocities calculated by lifting-line theory are employed to simplify the design procedure.

To determine the final blade geometry (pitch and camber distributions), lifting-line theory is not adequate. Lifting-surface theory needs to be used to incorporate three-dimensional effects of the flow field into the geometry of the design.

All the design codes described above are based on potential flow theory even though the effect of viscous drag has been incorporated into the force calculations. Boundary layer calculations need to be performed to ensure that the flow does not separate along the blade. The viscous drag has been calculated using the following empirical formula.

7

$$C_D = C_f(1 + 1.25(t/c) + 125(t/c)^4) \qquad (14)$$

where C_f is the skin friction coefficient of a smooth plate, and t/c is the section thickness to chord ratio. The value of C_f varies from 0.004 to 0.008 for corresponding blade section Reynolds numbers between 10^8 and 10^6.

Cavitation problems such as blade erosion and thrust breakdown are detrimental to ship performance. Cavitation performance can be improved by varying blade thickness, chord distribution, and blade loading, which in turn also affect the strength and the propulsive performance. Due to the differences in blade numbers and rotational speeds between the rotor and the vane wheel, the mutual interaction velocities between the two components need to be treated as an unsteady flow both in space and in time. A methodology which can handle the circumferential variations of the mutual interaction velocities for the vane-wheel propulsors must be developed.

By assuming that the blades could be treated as cantilever beams with variable cross section, the blade stress levels at the design point for both the rotor and the vane wheel were calculated using simple beam theory. However, to have a more accurate analysis for the full power ahead and the backing conditions, a finite element analysis is required.

The vane-wheel propulsor design needs to be analyzed using lifting-surface codes to determine the steady force produced by the propulsor. The fluctuating forces and moments also need to be computed. If the unsteady shaft forces and moments are below the allowable maximum unsteady forces and moments, the design is complete, otherwise, the skew distribution of the rotor needs to be adjusted to minimize the unsteady forces. Again, unsteady force calculations for vane-wheel propulsors must rely on methodology which can handle the variations of the mutual interactions between rotor and vane wheel. To obtain the most accurate results, the interaction velocities must be treated as unsteady. This is beyond the state of the art at the present time.

A VANE-WHEEL PROPULSOR DESIGN

In this section, a detailed design will be discussed using the design methodology described in the previous section. Since the present design is for uniform flow, some of the design stages will be skipped.

Design Requirements

The vane-wheel propulsor is designed for the operating condition of the AO-177 JUMBO at 10.61m/sec, and with a rotor rotational speed of 100 rpm. The rotor diameter and blade number were determined to be 6.4m and 5, respectively, based on the previous single-screw propeller design for the AO-177 JUMBO in the hull wake. To produce the same thrust, the vane-wheel propulsor designed for uniform flow maintains the same thrust loading coefficient, C_{th}, as the AO-177 JUMBO propulsor in the hull wake.

In order to obtain the highest possible propulsive efficiency, in the present study, the vane-wheel diameter and rotational speed were chosen as 1.3 times the rotor diameter and 0.40 of the rotor rotational speed, respectively. The vane-wheel blade number was chosen as 9. The 5 by 9 blade number may be a speculated combination in terms of unsteady forces between the rotor and vane

8

wheel because the second multiple of the rotor blade rate minus one is the vane-wheel blade rate. This may excite side forces and moments. However, there is no evidence to show that this combination is inappropriate at the present time. The distance between the reference line of the rotor and vane wheel was chosen as a quarter of the rotor diameter.

Preliminary Design

The details of the lifting-line calculations are discussed in this section. The optimum circulation of the vane-wheel propulsor is determined by the variational approach which was described previously. Fig. 3 shows the optimum and the unloaded circulations for the rotor of the vane-wheel propulsor. The reason for unloading the blade tip is to reduce the tendency toward cavitation erosion near the tip. However, unloading the blade tip results in a reduction in propulsive efficiency. Similarly, the reason for unloading the blade root is to mitigate cavitation erosion near the root.

The single-screw propeller for AO-177 JUMBO in the hull wake was designed by Kim [9]. In the present study, the single-screw propeller has been redesigned for uniform flow at the operating condition of the AO-177 JUMBO propulsor for a fair comparison. The optimum and unloaded circulation distributions are shown in Fig. 3. In contrast to the single-screw propeller blade loading, the blade loading of the vane-wheel rotor is shifted inboard so that the axial kinetic energy losses can be reduced.

The turbine part of the vane-wheel propulsor is designed by imparting the same mass flow as is absorbed by the rotor. The radius of the turbine part is 0.93 of the rotor diameter using the mass conservation calculation. Fig. 4 shows the radial distribution of the optimum and the unloaded circulations for the vane wheel. In unloading the vane-wheel tip and hub, one has to consider maintaining zero torque on the vane wheel.

The chord distributions were chosen based on, cavitation, flow separation, and efficiency considerations. The thickness distribution was selected based on strength, cavitation, and the blade weight.

Since the vane-wheel propulsor is designed for uniform flow, cavitation calculations have been ignored in the present study.

Final Design

Lifting-surface design is the final design stage. The final pitch and camber distributions were determined from lifting-surface theories developed by Brockett [10], and by Greeley and Kerwin [11].

For marine propeller applications, the a = 0.8 meanline is a suitable chordwise loading distribution from cavitation and viscous flow points of view. NACA 16 and NACA 66 thickness distributions normally have low drag, and good cavitation features. For surface ship applications, the NACA 66 thickness distribution is generally selected.

As shown in Figs. 5 and 6, the final pitch and camber distributions for the rotor of the vane-wheel propulsor were calculated using Brockett's lifting-surface theory and Greeley and Kerwin's lifting-surface theory. Both the pitch and camber distributions from these two lifting-surface theories are similar except near the hub. In the present study, the results from Brockett's lifting-surface
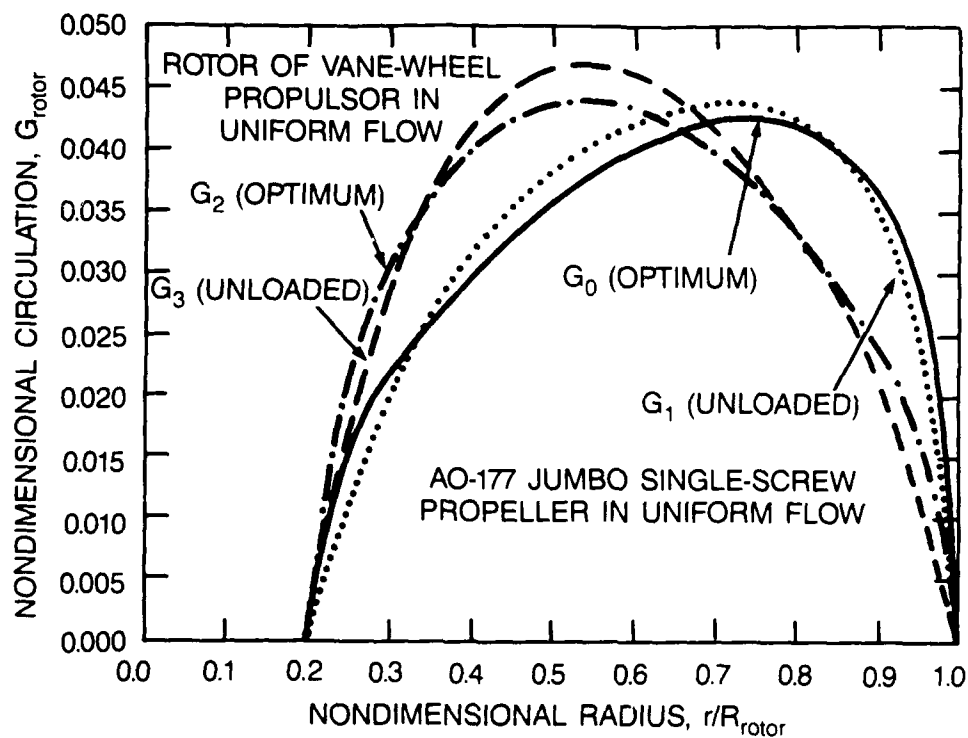
9

Fig. 3. Optimum and unloaded circulation distribution for the AO-177 JUMBO single-screw propeller and the rotor of vane-wheel propulsor in uniform flow.
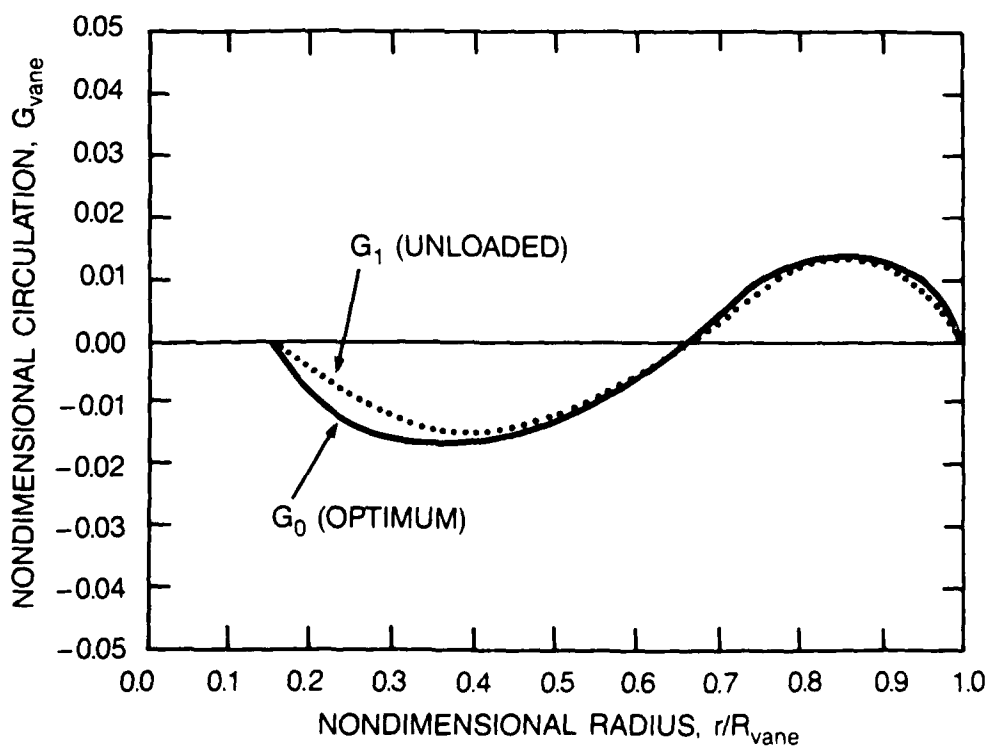

Fig. 4. Optimum and unloaded circulation distribution for vane wheel.
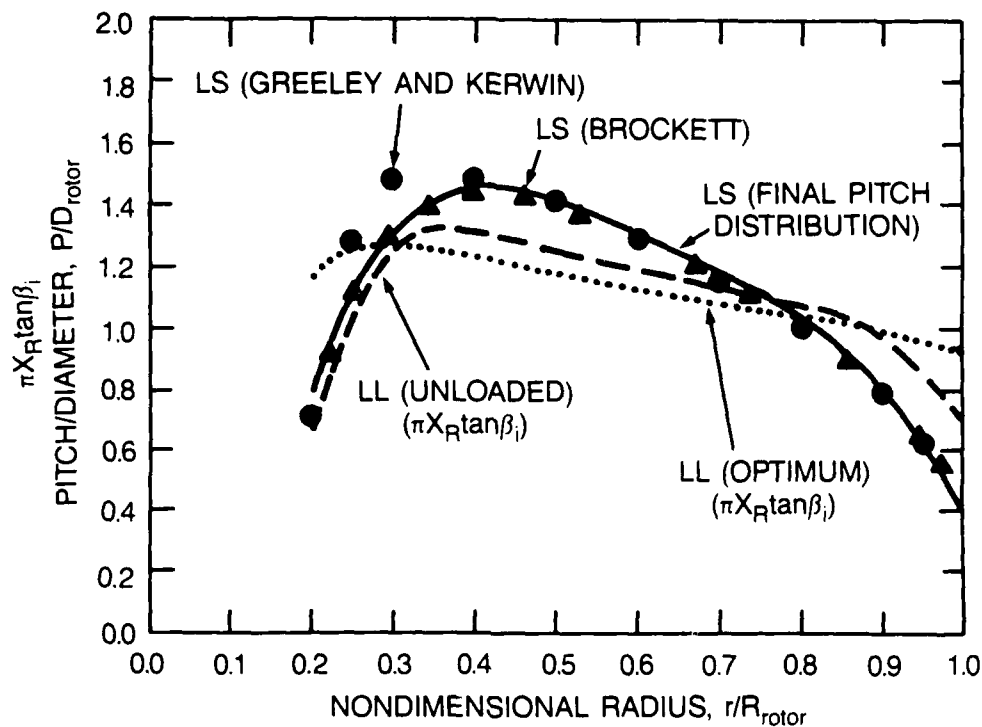
Fig. 5. Radial distribution of optimum and unloaded $\pi X_R \tan\beta_i$ and pitch/diameter ratio for rotor of vane-wheel propulsor.
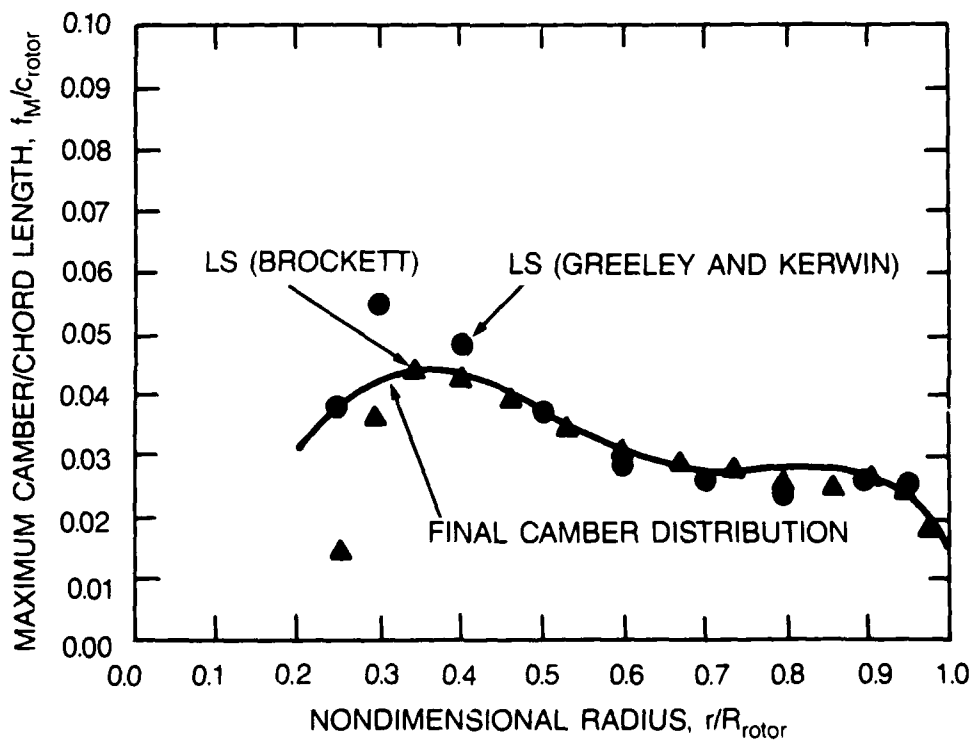

Fig. 6. Final maximum camber ratio distribution for rotor of vane-wheel propulsor.

11

theory were selected because they seemed more reasonable. A comparison between pitch from the lifting-surface calculation, and $\pi X_R \tan\beta_i$ is also shown in Fig. 5. It can be seen that the two curves are similar.

The hydrodynamic pitch angle and camber distribution for the vane wheel, also calculated by Brockett's lifting-surface theory and Greeley and Kerwin's lifting-surface theory are shown in Figs. 7 and 8, respectively. The hydrodynamic pitch angle and camber distribution from these two lifting-surface theories are similar. The comparison of the unloaded hydrodynamic pitch angle from the lifting-line and the lifting-surface designs is also shown in Fig. 7. It can be seen that the two curves are very similar.

Performance Prediction

The vane-wheel propulsor design was analyzed using the lifting-surface theory developed by Greeley and Kerwin [11]. This lifting-surface theory computes the design and the off design steady forces on the components of the vane-wheel propulsor.

At the design point, the rotor thrust and torque predictions are almost identical to the design values. The vane-wheel torque is not zero at the design rpm. However, by using a rpm 0.2 higher than the design rpm, the torque approaches zero, and the thrust matches the design. A summary of the vane-wheel propulsor design is given in Table 1. Performance predictions and open water tests for the vane-wheel propulsor are shown in Table 2. The results show that the performance predictions agree well with the measurements.

The unsteady force calculations for the vane-wheel propulsor have been ignored because the present design is for uniform flow. However, the outflow from the rotor does provide a non-uniform inflow for the vane wheel. Due to the light loading on the rotor, this is not considered to be significant. Photos of the final vane-wheel propulsor geometry are shown in Fig. 9.

Table 1. Vane-wheel propulsor design — Summary.

	Rotor (given)	Vane Wheel (calculated)
$J_s{}^*$	0.771	1.928
Geometry		
Diameter (m)	6.400	8.321
Number of Blades	5	9
Expanded Aera Ratio	0.770	0.649
Skew (deg)	40	0
Blade sections	NACA 66 (DTMB Modified) Thickness NACA a = 0.8 Meanline	
Axial Spacing (m)	1.600	
Cth	1.311	

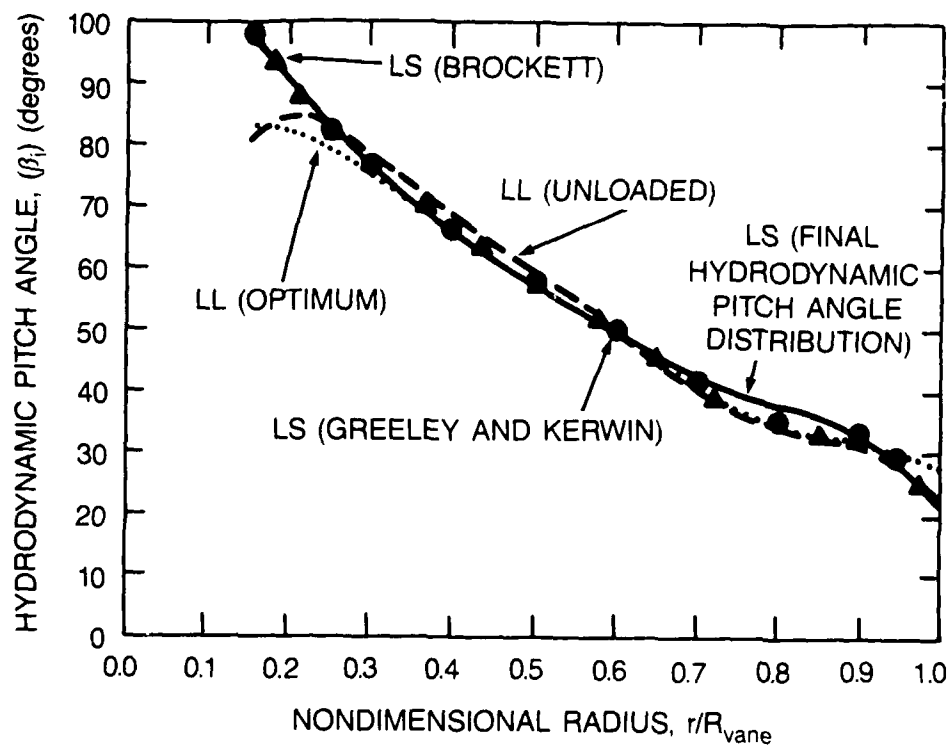*All results for vane wheel are based on rotor diameter.

12

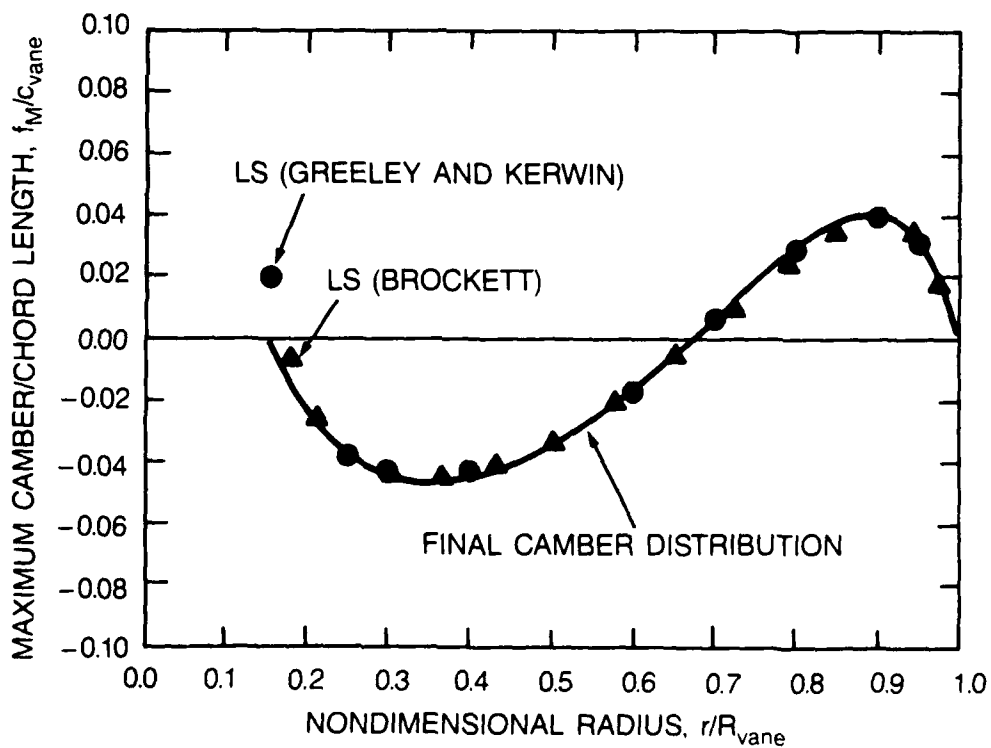**Fig. 7.** Optimum and unloaded hydrodynamic pitch angle for vane wheel.

Fig. 8. Final maximum camber ratio distribution for vane wheel.

13

Table 2. Predicted and measured performance of vane-wheel propulsor.

	Prediction		Experiment	
	Design (des. J)	Inverse Calculation (const. Cth)	Vane Wheel as a Windmill (des. J)	Vane-Wheel Torque Forced to be Zero (const. Cth)
Rotor				
K_T	0.2883	0.2883	0.2940	0.2950
K_Q	0.0546	0.0546	0.0552	0.0554
rpm	100	100	100	99.23
Vane Wheel				
$K_T{}^*$	0.0216	0.0239	0.0150	0.0159
$K_Q{}^*$	−0.0015	−0.0004	−0.0072	0.0004
rpm	40	40.2	40	40.16
Vane-Wheel Propulsor				
$J_s{}^*$	0.771	0.771 (−0.8%)	0.771	0.777
K_T	0.3099	0.3120 (+0.4%)	0.3090	0.3109
$K_Q{}^{**}$	0.0546	0.0546 (−1.4%)	0.0552	0.0554
N_R/N_V	2.5	2.488 (+0.7%)	2.5	2.471
η†	0.697	0.701 (+1%)	0.687	0.692
Power red.††	—	8%	—	9.5%

* All results for vane wheel are based on rotor diameter.
** This value does not include the vane-wheel contribution.

†
$$\eta = \frac{K_T}{K_Q} \frac{J_s}{2\pi}$$

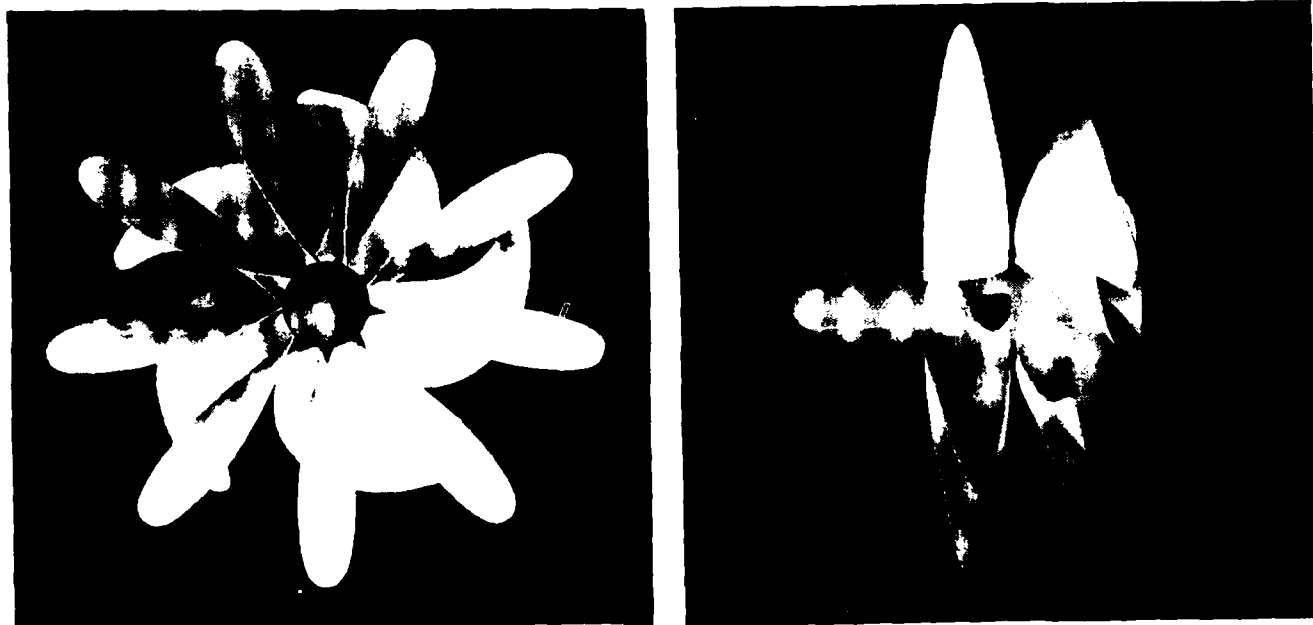†† Based on the open-water tests for AO-177 JUMBO single screw propeller.

Fig. 9. Final geometry for vane-wheel propulsor.

14

CONCLUSIONS AND RECOMMENDATIONS

A design methodology for vane-wheel propulsors has been developed using the principles of momentum, mass, and circulation conservation. Momentum conservation requires that the net force generated by the vane-wheel propulsor be balanced by the bare body drag and the losses due to hull-propulsor interactions. Mass conservation determines the distribution of vane-wheel circulation once the rotor circulation distribution is specified. Circulation conservation determines the magnitude of the vane-wheel circulation to ensure zero torque on the vane wheel. The mutual interaction velocities between the rotor and the vane wheel were predicted using lifting-line theory.

A vane-wheel propulsor was designed for uniform flow at the design conditions of the AO-177 JUMBO naval auxiliary. For the highest efficiency, the vane-wheel diameter and the rotational speed were chosen as 1.3 of the companion rotor diameter and 0.40 of the rotor's rotational speed. The vane-wheel blade number was chosen as 9. Open water test results show that the performance predictions agree with the measurements very well. The shaft horsepower with vane wheel is 9 percent lower than without. The conclusions from this paper are as follows.

(1) The present design methodology is an appropriate procedure for vane-wheel propulsor design.

(2) The mutual interaction velocities between the rotor and vane wheel play important roles in the vane-wheel propulsor design. If the rotor is heavily loaded, the mutual interaction velocities should probably be predicted using the lifting-surface theory.

(3) In the present study, the shaft horsepower of the vane-wheel propulsor is 9 percent lower than that of a single screw propeller. Normally, a shaft horsepower reduction of about 10 percent is expected for a vane-wheel propulsor. This improvement depends on the specific loading conditions (normally $C_{th} > 2.0$ [12]) and the type of the ship. Therefore, it is very important to choose a suitable ship for the application of the vane-wheel propulsor concept. In this case, we had to choose an extreme increase in diameter to obtain expected shaft horsepower reduction. With practical diameter constraints, a vane-wheel propulsor would not be a good candidate propulsor for the AO-177 JUMBO.

There are several recommendations for further study of this topic.

(1) The present design method does not include the effect of the hub on the loading distribution of the rotor and vane wheel. This is an important factor which should be included in the design method, particularly in light of the fact that the presence of the vane wheel behind the rotor tends to move the rotor's loading inboard.

(2) A method for predicting the circumferential variations in the mutual interaction velocities for the vane-wheel propulsor is necessary. Such calculations are critical to the prediction of cavitation and unsteady forces, particularly for the vane wheel.

ACKNOWLEDGMENTS

REFERENCES

1. Grim, O., "Propeller und Leitrad," *Jahrbuch der Schiffbautechnischen Gesellschaft,* Band 60, (1966).
2. Grim, O., "Propeller and Vane Wheel," *Journal of Ship Research,* Vol. 24, No. 4, (1980).
3. Kehr, Y.-Z., "Hydrodynamische Analyse des Leitrads," Vom Fachbereich fur Verkehrswesen der Technischen Universitat, Doktor-Ingenieur genehmigte Dissertation (1986).
4. Blaurock, J., "Propeller Plus Vane Wheel, an Unconventional Propulsor System," International Symposium on Ships Hydrodynamics and Energy Saving, El Pardo, (1983).
5. Van Beek, T. and B.V. Lips, "Hydrodynamic Features of the New QE-2 Propulsion System," 6th LIPS Propeller Symposium, (1986).
6. Huang, T.T. and N. Groves, "Effective Wake: Theory and Experiment," the 13th Symposium on Naval Hydromechanics, (1980).
7. Kerwin, J.E., W.B. Conney and C.-Y. Hsin, "Optimum Circulation Distributions for Single and Multiple-Component propulsors," 21st American Towing Tank Conference, National Academy Press, p.53-62, (1986).
8. Chen, B. Y.-H. and A.M. Reed, "A Lifting-Surface Program for Contrarotating Propellers," Symposium on Hydrodynamic Performance Enhancement for Marine Applications, NUSC, Newport, RI, (1988).
9. Kim, K.-H., "Propeller Design for Naval Auxiliary AO-177 JUMBO," DTNSRDC Ship Hydromechanics Department Report, DTNSRDC/SHD-1227-01, (1987).
10. Brockett, T.E., "Lifting Surface Hydrodynamics for Design of Rotating Blades," Propellers' 81 Conference, SNAME, Virginia Beach, VA (1981).
11. Greeley, D.S. and J.E. Kerwin, "Numerical Methods for Propeller Design and Analysis in Steady Flow," *Transactions SNAME,* Vol. 90, p.415-453, (1982).
12. vom Baur, M. and K.J. Meyne, "The Grim-Wheel − Reports and Experiences," HANSA Report, (1984).

APPENDIX

PLL AND LL106 FOR SINGLE SCREW PROPELLER

A comparison of the optimum circulations from PLL, developed by Kerwin et. al, and LL106, developed by Caster et. al,* is shown in Fig. 10. As stated in the text, the optimum circulation from PLL is derived from the variational approach, that of LL106 is from a Lerbs optimum circulation approximation. It can be seen that the circulation distributions from PLL and LL106 are very similar. The thrust and torque coefficients, and the open water efficiency predicted by the two programs are almost identical. Fig. 11 shows that the hydrodynamic pitch from the two programs is also similar. Based on the above comparisons, the accuracy of PLL for a single-screw propeller is very good.

INDUCED VELOCITIES FROM LIFTING-LINE AND LIFTING-SURFACE THEORIES

Figure 12 shows the radial distribution of the axial velocity, u_{a21}, induced by the rotor on the vane wheel. It shows that the difference between the lifting-line and the lifting-surface theories is small except near the hub because the lifting-surface theory takes the hub effects into account.** The variations in the radial velocity, u_{r21}, induced by the rotor on the vane wheel is shown in Fig. 13. The magnitude of the radial velocity for the lifting-line theory is equal to zero because the lifting-line theory does not account for the radial induced velocity. As Fig. 14 shows, the tangential velocity, u_{t21}, induced by the rotor on the vane wheel for both theories are similar except near the hub. Since the velocities induced by the rotor on the vane wheel are similar, the induced velocities calculated by lifting-line theory are employed to simplify the design procedure.

PARAMETRIC STUDY FOR A VANE-WHEEL PROPULSOR

The purpose of this study is to secure the highest possible propulsive efficiency for the vane-wheel propulsor design.

Parametric calculations for a single-screw propeller on AO-177 JUMBO in uniform flow were performed, and are shown in Fig. 15. This figure shows that the optimum rotational speed is about 100 rpm with a propeller diameter of 21.0 ft (6.4 m), and 5 blades.

As for the vane-wheel propulsor, the efficiency versus the ratio of the rotational speed for various vane-wheel diameters and fixed vane-wheel blade number is shown in Fig. 16. This figure indicates that the larger the vane-wheel diameter, the higher the efficiency which can be achieved. This is due to the fact that the larger vane-wheel diameter provides a larger portion of the rotor over which the blade loading will be reduced. Plots of efficiency versus the ratio of the rotational speed of the vane wheel and the rotor with various vane-wheel blade numbers are shown in Fig. 17, for a fixed vane-wheel diameter. These plots show that the higher the blade number, the higher the efficiency. This is due to the fact that the loading on a single blade is lower for the vane-wheel

---

*Caster, E., et. al, "A Lifting-Line Computer Program for Preliminary Design of Propellers," DTNSRDC Ship Performance Department report, DTNSRDC/SPD-595-01 (1975).

**The current PLL code includes the capability of the hub image effects. However, it was not available when this design was completed.
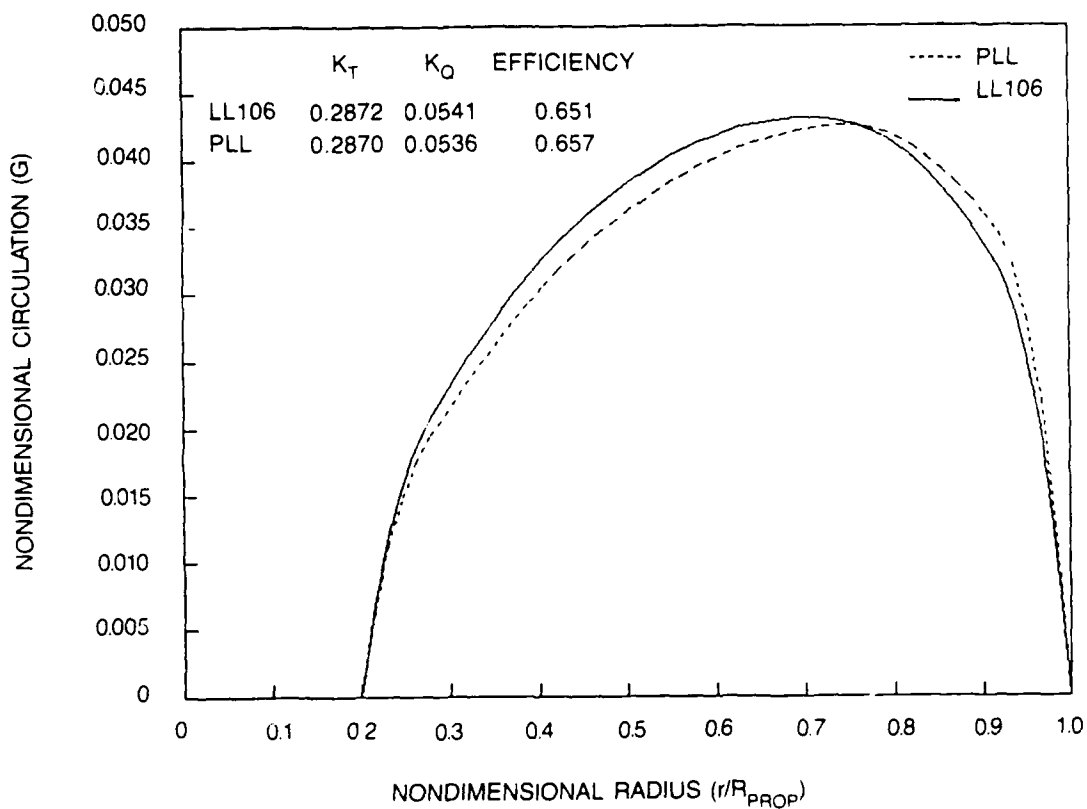
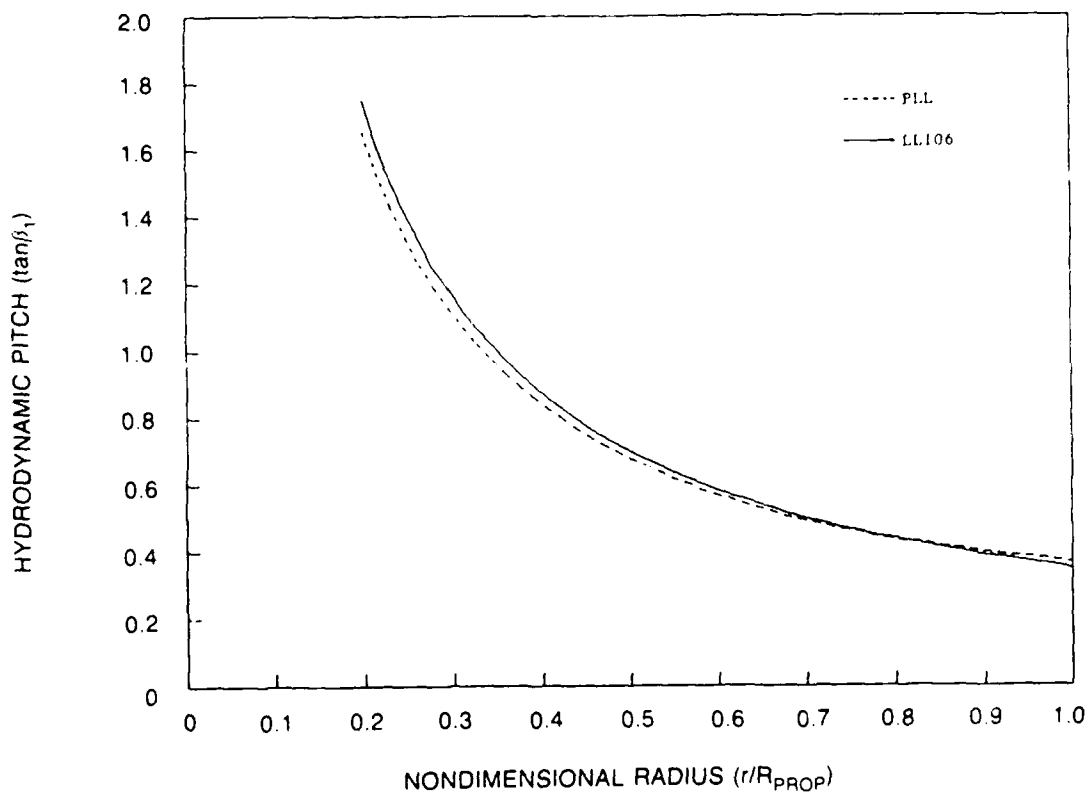**Fig. 10.** Comparison of optimum circulation distribution from PLL and LL106.

Fig. 11. Comparison of hydrodynamic pitch from PLL and LL106.

18

Fig. 12. Radial distribution of axial veloc 'y induced by rotor on vane wheel from lifting-line and lifting-surface theories.
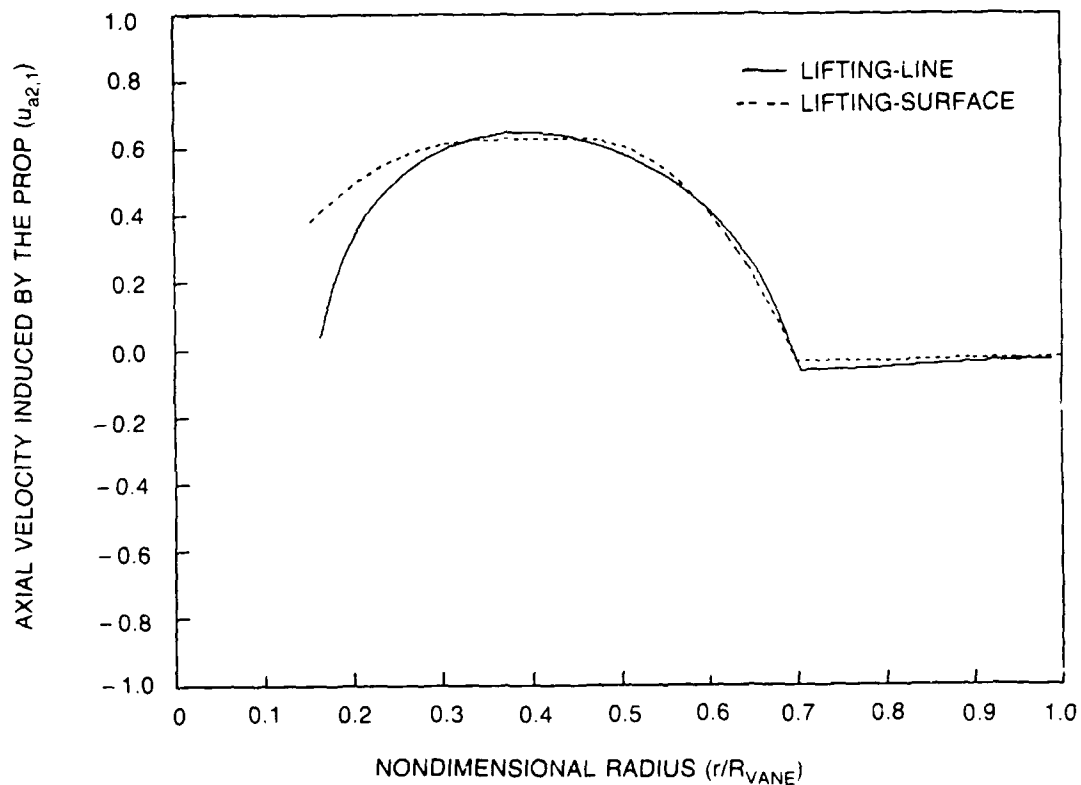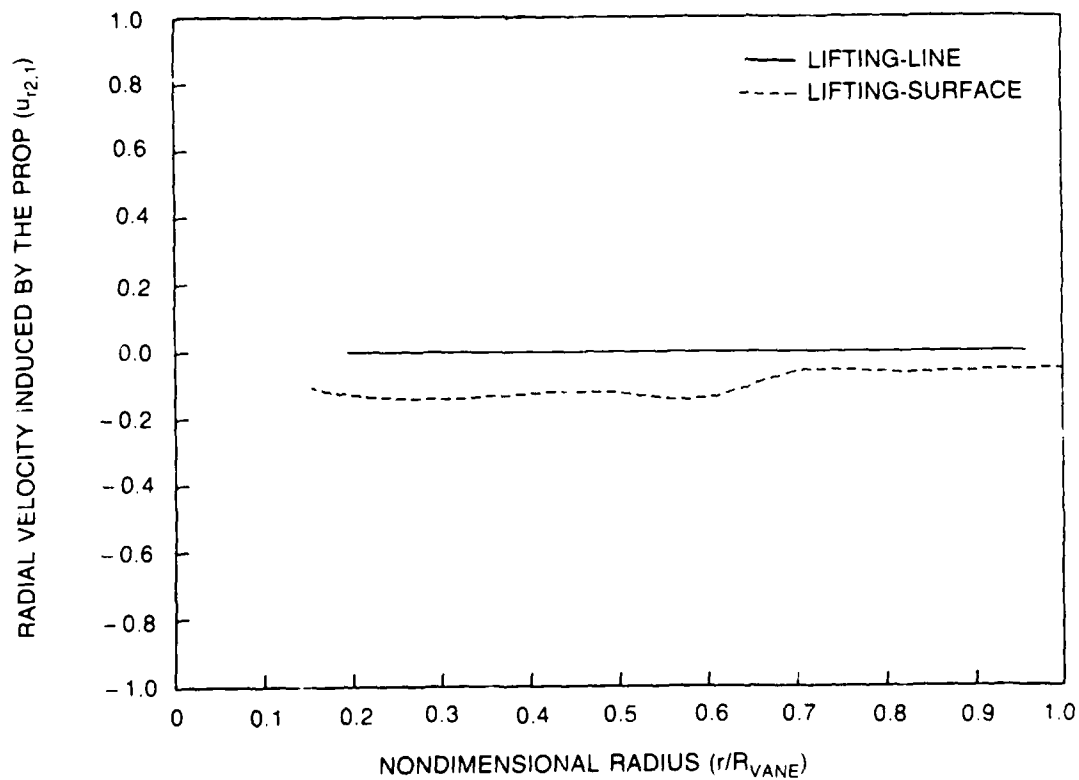

Fig. 13. Radial distribution of radial velocity induced by rotor on vane wheel from lifting-line and lifting-surface theories.

19
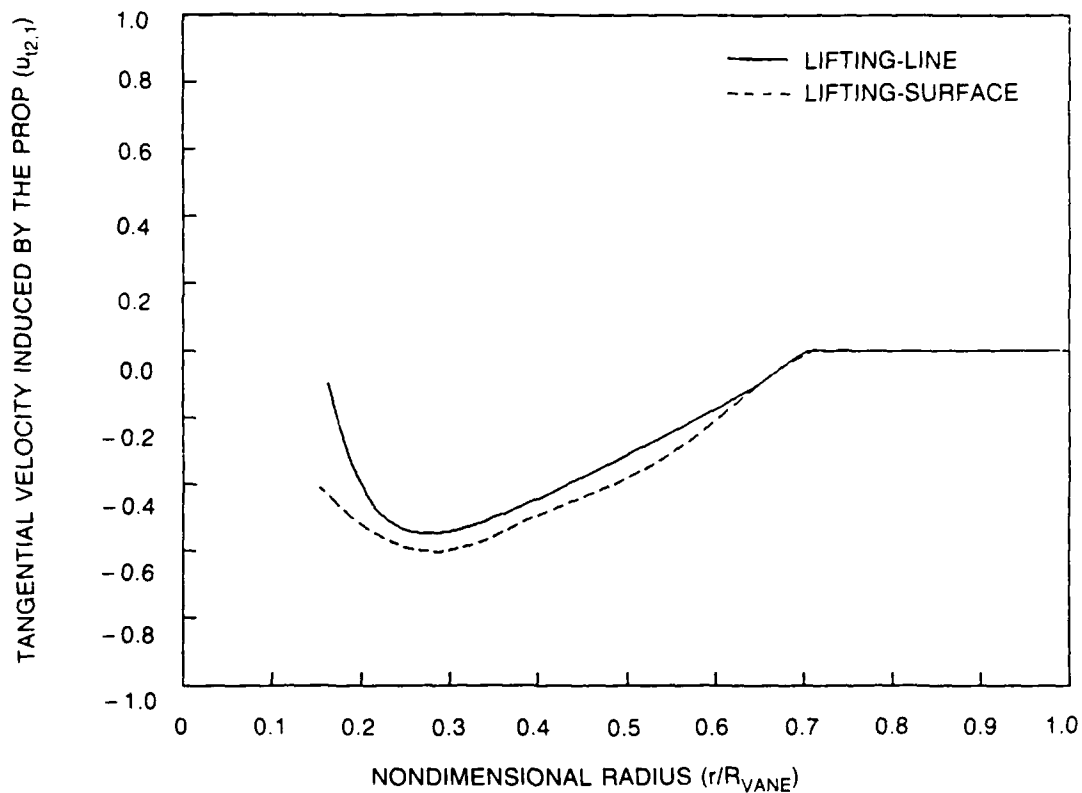
Fig. 14. Radial distribution of tangential velocity induced by rotor on vane wheel from lifting-line and lifting-surface theories.
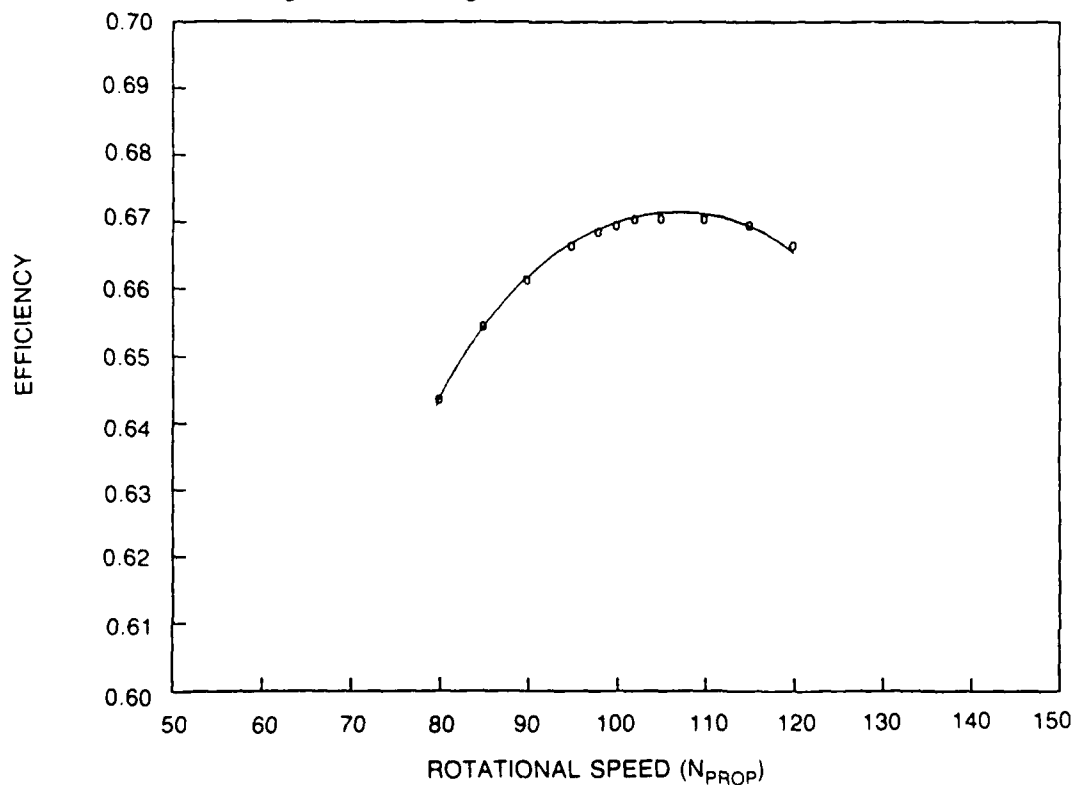
Fig. 15. Propeller efficiency versus rotational speed for AO-177 JUMBO single-screw propeller in uniform flow.

20
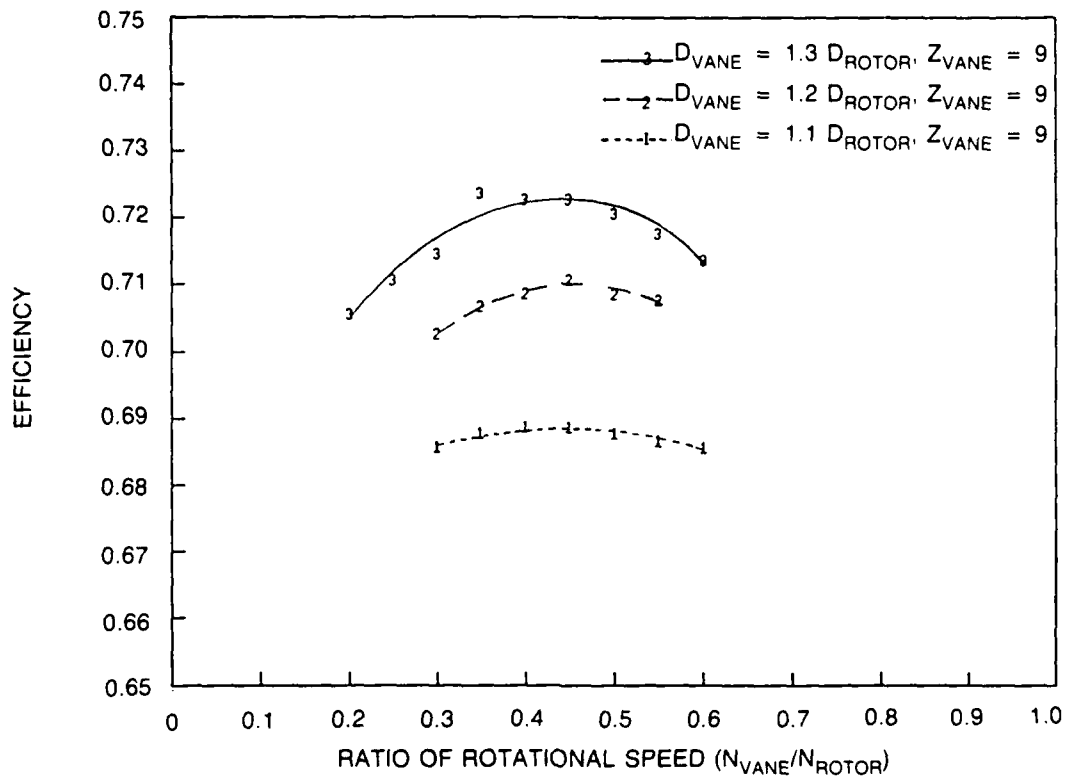
Fig. 16. Propulsor efficiency versus ratio of rotational speed for various vane-wheel diameters and fixed vane-wheel blade number.
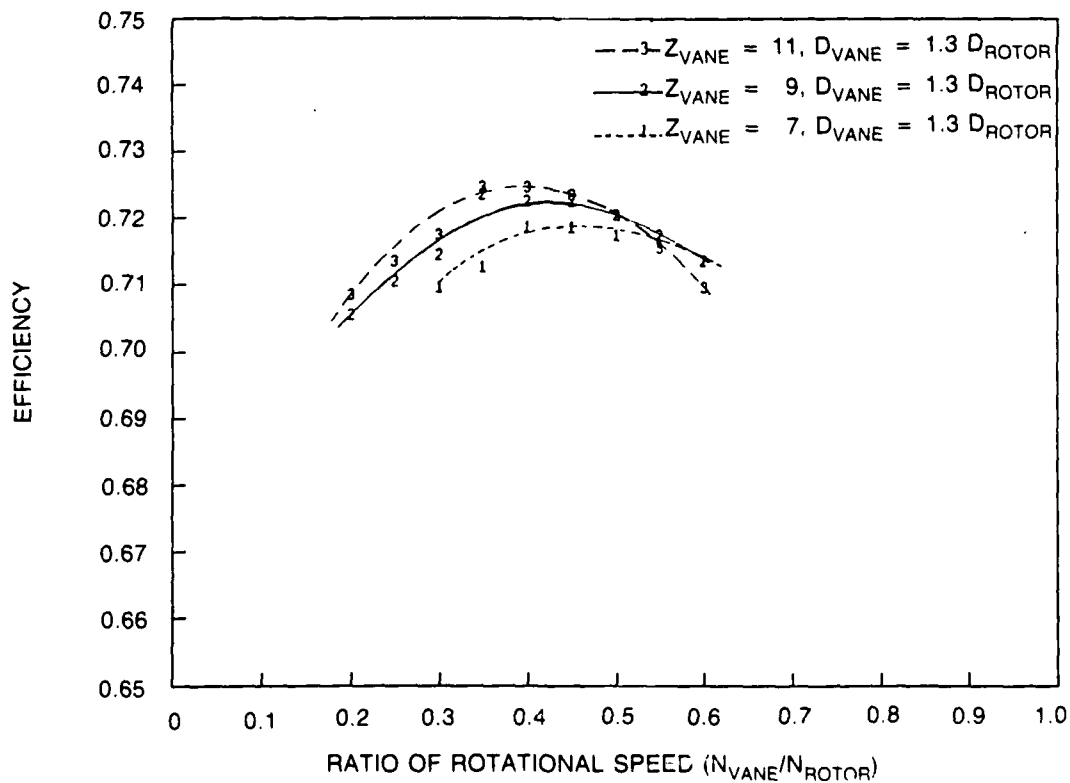
Fig. 17. Propulsor efficiency versus ratio of rotational speed for various vane-wheel blade numbers and fixed vane-wheel diameter.

21

with a large blade number than that for the vane-wheel with a small blade number. The optimum rotational speed of the vane wheel is 30 to 50 percent of that of the rotor.

GEOMETRIC SPECIFICATIONS FOR A VANE-WHEEL PROPULSOR

Chord distribution for the rotor of the vane-wheel propulsor, the single-screw propeller, and the vane wheel is given in Fig. 18. The maximum chord of the rotor was shifted inboard to match the maximum circulation. In addition, the expanded area ratio (EAR) was reduced to get better efficiency, the EAR was limited by cavitation considerations. The minimum EAR was calculated using both Burrill's and Keller's cavitation criteria.

The vane-wheel propulsor thickness distribution is given in Fig. 19. A comparison of the thickness distribution of the rotor with that of the AO-177 JUMBO single-screw propeller shows that both thickness distributions are very similar.

As shown in Fig. 20, the rotor of the vane-wheel propulsor was designed with the same skew distribution as the single-screw propeller for the AO-177 JUMBO. The vane wheel was designed with zero skew. Both the rotor and the vane wheel were designed with zero total rake. In other words, the rotor actually has negative rake to offset the skew induced rake.

The stress distributions for the rotor and the vane wheel are given in Fig. 21. The maximum stresses are well below the allowable stress of 12,500 psi for Nickel-Aluminum-Bronze.

FINAL VANE-WHEEL PROPULSOR GEOMETRY

The final geometric specifications of the vane-wheel propulsor, including the details of the leading and the trailing edges were computed using the computer code, XYZPROP, developed by Brockett.* All the vane-wheel propulsor geometric data such as chord length, thickness, skew, pitch, and camber distributions need to be faired before they can be input to XYZPROP. A list of chord length, thickness, skew, pitch and camber distributions for the vane-wheel propulsor is given in Table 3.

OPEN-WATER TESTS FOR A VANE-WHEEL PROPULSOR

Model rotor and vane wheel (DTRC propellers 5080 and 5081) were manufactured based on the final design geometry shown in Table 3. Three sets of open-water tests were carried out with the vane wheel mounted on the contrarotating (CR) propeller dynamometers: the vane-wheel as a windmill, the vane-wheel with zero torque, and the rotor without the vane wheel.

Figure 22 presents test results based on the experiment wi.h zero vane-wheel torque for different advanced coefficients. The open-water performance for the wake-adapted single screw propeller of AO-177 JUMBO is also shown in the same figure. In general, the accuracy of the experimental measurements with the CR propeller dynamometers is ±2 percent on thrust and torque.

---

*Brockett, T.E., "Analytical Specification of Propeller Blade-Surface Geometry," DTNSRDC Ship Performance Department report, DTNSRDC/SPD-699-01 (1976).

Table 2 shows the predicted and measured performance of vane-wheel propulsor design. For design condition at design advance coefficient, test results show that the vane wheel can not obtain zero torque as it is predicted. However, for the inverse calculation at constant C_{th}, test results indicate that the vane wheel achieved zero torque at the same rotational speed as the prediction. The rotor rotational speed from the prediction is 0.8 rpm lower than that from the experiment.

At the design C_{th}, the measured advance coefficient is 0.8 percent higher than that for which the propulsor was designed. At this same condition, the unit thrust prediction is 0.4 percent higher than the measurement and the unit torque prediction is 1.4 percent lower. The predicted rotational speed ratio is 0.7 percent and the predicted efficiency is 1.0 percent higher than that from the experiment. Overall the predicted values agree well with the experimental measurements, and in general are within the accuracy of the experimental measurements.

Table 3. Final design geometry for vane-wheel propulsor.

(a) Rotor

r/R	c/D	P/D	i_T/D	θs	t/c	f_M/C
0.2000	0.3178	0.7856	0.0000	0.000	0.19040	0.03027
0.2500	0.3315	1.1051	0.0000	−0.200	0.17430	0.03695
0.3000	0.3413	1.3152	0.0000	−0.300	0.15860	0.04200
0.4000	0.3499	1.4648	0.0000	−0.100	0.13010	0.04371
0.5000	0.3461	1.4196	0.0000	1.200	0.10750	0.03760
0.6000	0.3340	1.3118	0.0000	4.400	0.09090	0.03160
0.7000	0.3156	1.1822	0.0000	9.800	0.07840	0.02849
0.8000	0.2861	1.0245	0.0000	17.700	0.06760	0.02808
0.9000	0.2195	0.8018	0.0000	28.900	0.05724	0.02750
0.9500	0.1448	0.6330	0.0000	35.400	0.05210	0.02363
1.0000	0.0000	0.3998	0.0000	40.000	0.04690	0.01650

(b) Vane Wheel

r/R	c/D	P/D	i_T/D	θs	t/c	f_M/C
0.1538	0.1483	97.8175	0.0000	0.000	0.1360	0.0000
0.2500	0.1501	83,6533	0.0000	0.000	0.1242	−0.0367
0.3000	0.1508	77.4890	0.0000	0.000	0.1184	−0.0441
0.4000	0.1515	67.2547	0.0000	0.000	0.1076	−0.0437
0.5000	0.1506	58.1760	0.0000	0.000	0.0980	−0.0328
0.6000	0.1472	49.8808	0.0000	0.000	0.0898	−0.0149
0.7000	0.1393	43.0000	0.0000	0.000	0.0828	0.0080
0.8000	0.1249	37.8251	0.0000	0.000	0.0766	0.0299
0.9000	0.1011	32.9470	0.0000	0.000	0.0707	0.0408
0.9500	0.0797	28.6783	0.0000	0.000	0.0678	0.0313
1.0000	0.0000	21.7895	0.0000	0.000	0.0649	0.0045

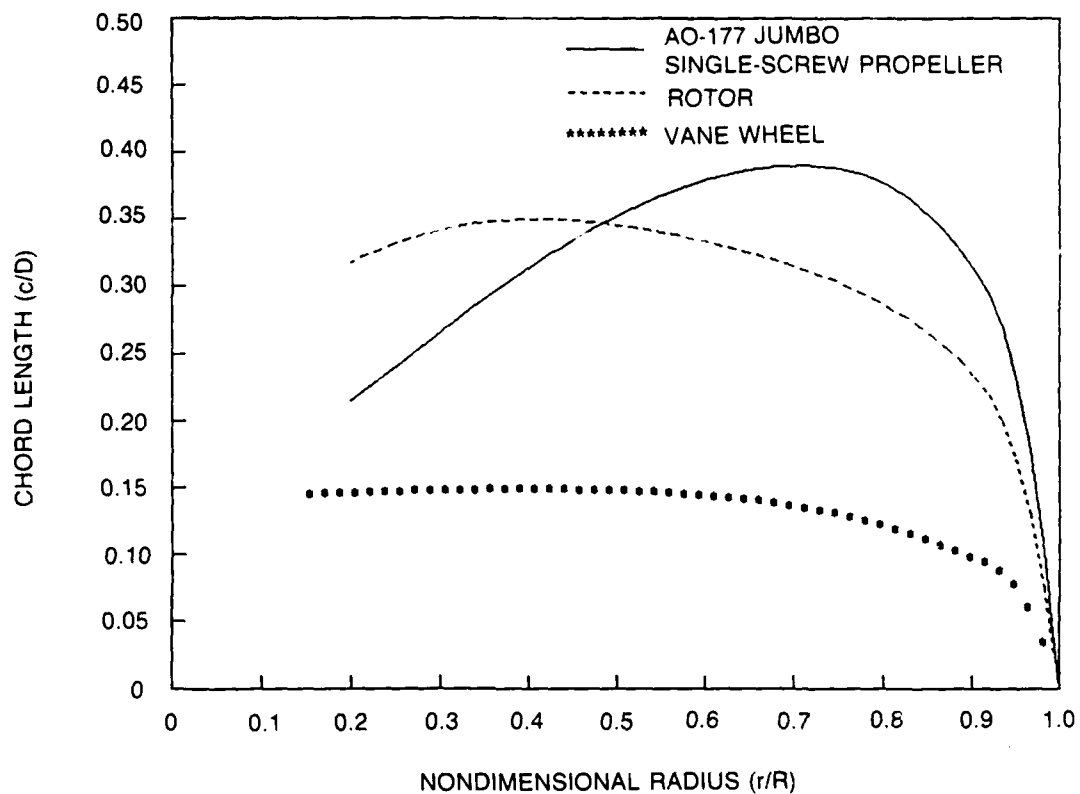**Fig. 18.** Radial distribution of chord length for the AO-177 JUMBO and the rotor and the vane wheel.
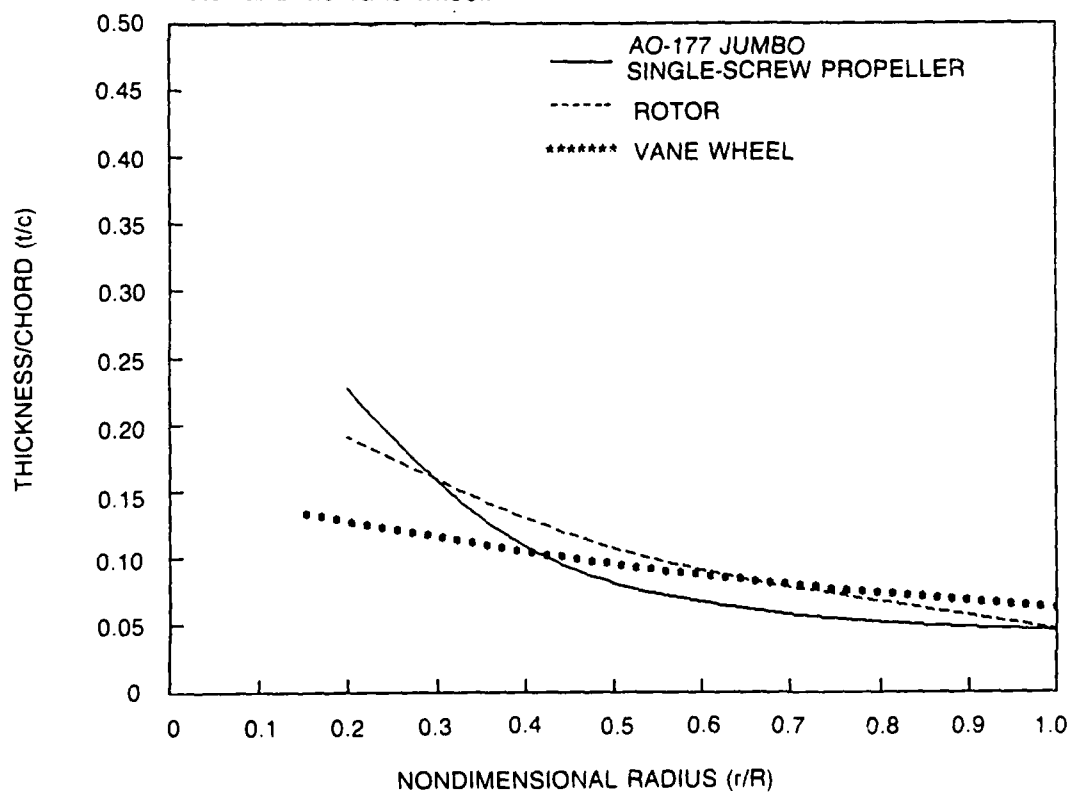

Fig. 19. Radial distribution of thickness for the AO-177 JUMBO and the rotor and the vane wheel.
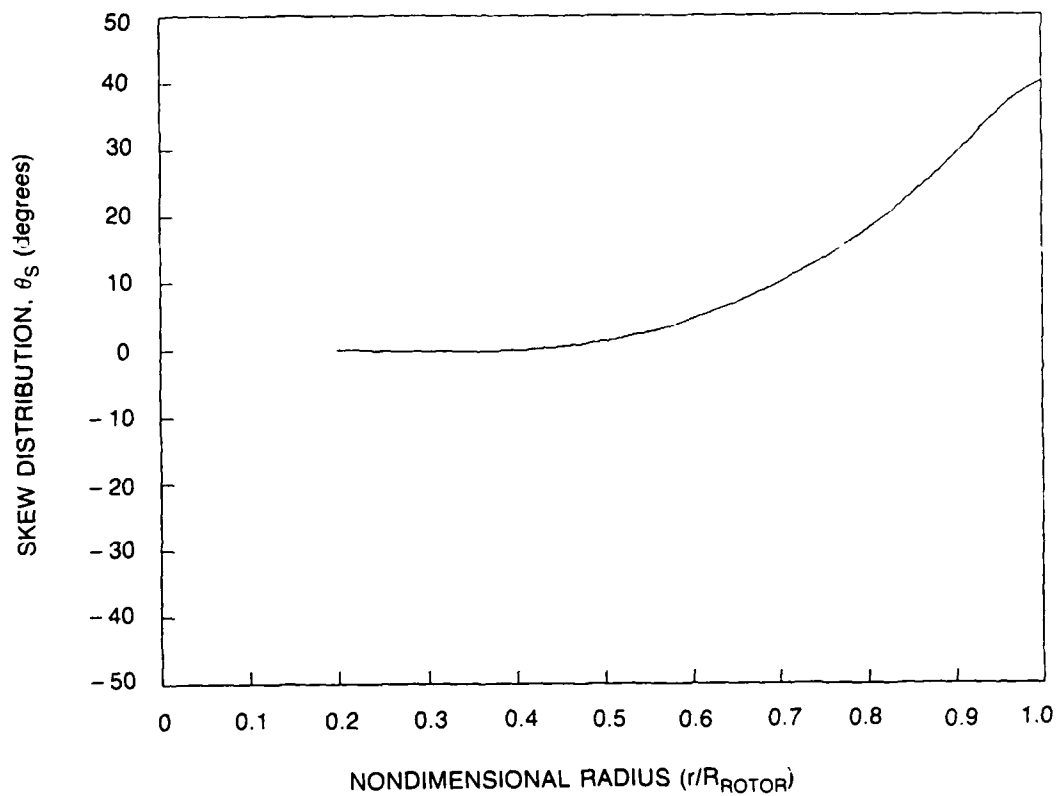
24

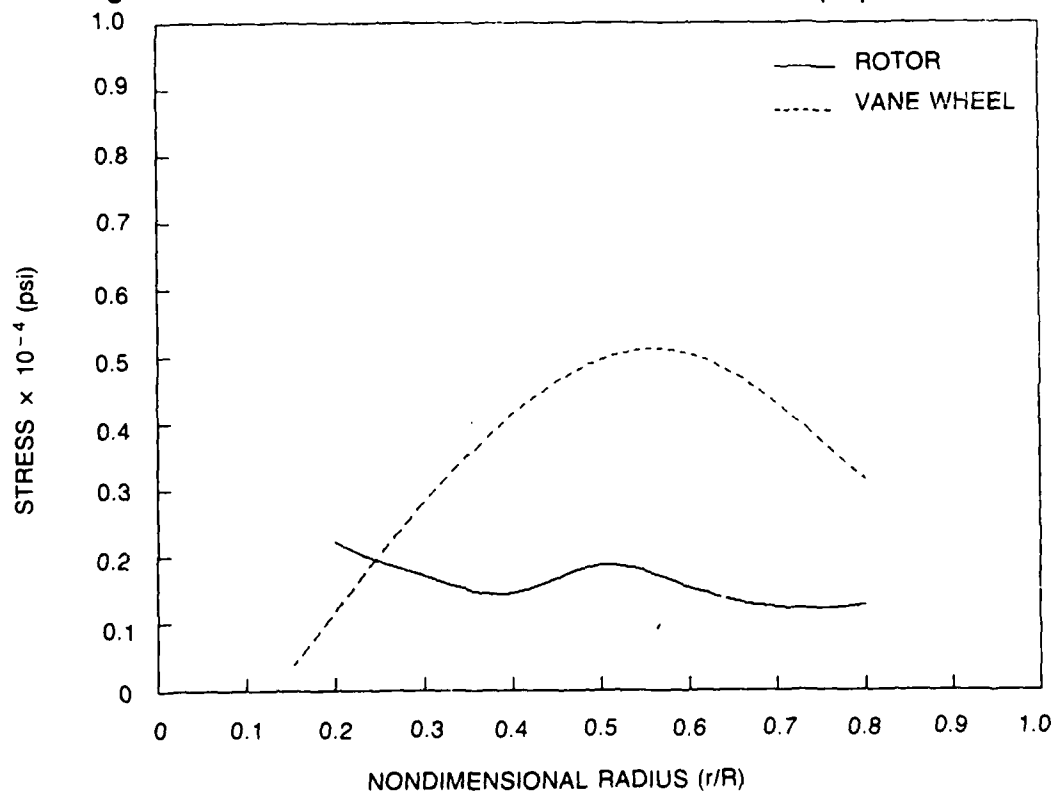**Fig. 20.** Radial distribution of skew for rotor of vane-wheel propulsor.

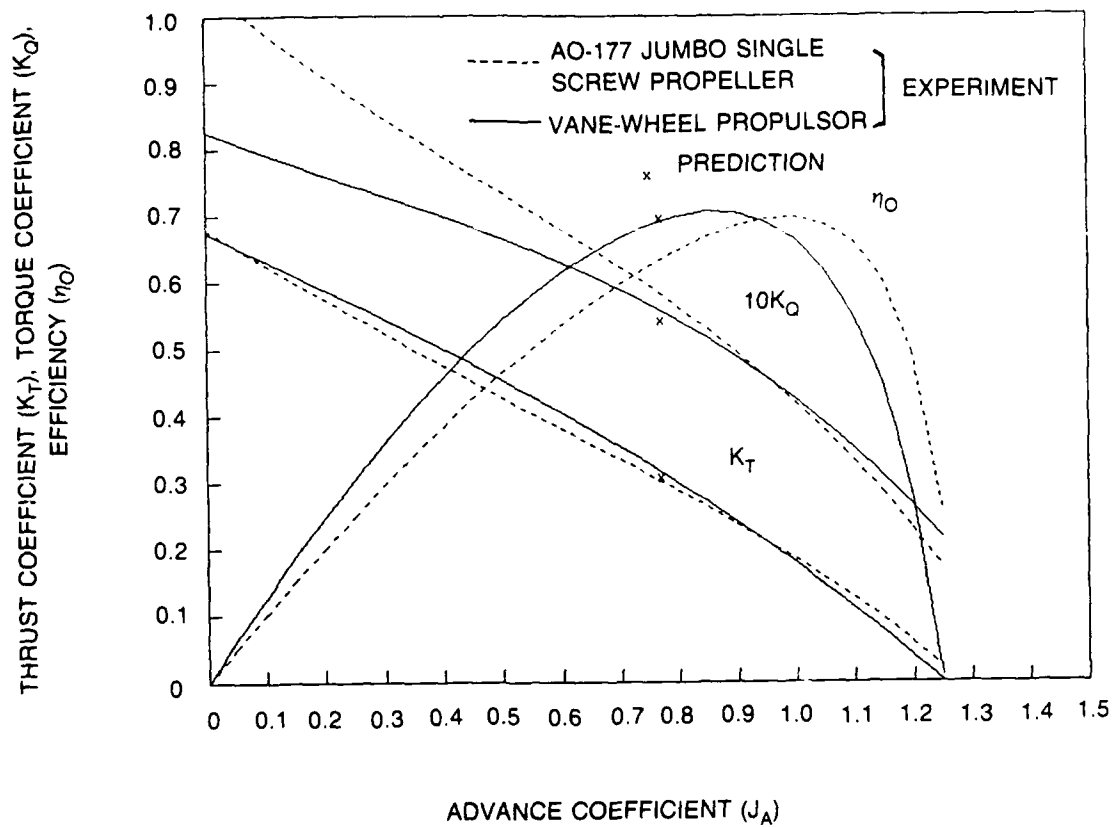**Fig. 21.** Radial distribution of stress for rotor and vane wheel.

25

Fig. 22. Open-water tests for vane-wheel propulsor.

26

INITIAL DISTRIBUTION

Copies		Copies	
1	Army Chief of Res & Dev		NAVSEA (Continued)
		1	SEA 56XN
1	AER&DL	1	PMS-383
		1	PMS-392
4	CHONR	1	PMS-396
	1 Lib	1	PMS-399
	1 Code 11	1	PMS-400
	1 Code 21	1	SEA Tech Rep
	1 Code 12		Bath, England
		2	DET Norfolk (Sec 6660)
4	ONR Boston		
		2	MMA
4	ONR Chicago		1 Lib
			1 Maritime Res Cen
4	ONR London, England		
		12	DTIC
1	NRL		
		2	HQS COGARD
2	USNA		
	1 Lib	1	US Coast Guard (G-ENE-4A)
	1 Johnson		
		1	LC/SCI & Tech Div
1	NAVPGSCOL Lib		
		1	NASA STIF
1	NROTC & NAVADMINU, MIT		1 Dir Res
1	NADC	1	NSF Eng Div/Lib
4	NOSC	1	DOT Lib
	1 1311 Lib		
	1 6005	2	U. Cal Berkeley/Dept Name
	1 13111 Lib		1 Name Lib
	1 Mautner		1 Webster
1	NSWC	1	U. Mississippi Dept of M.E.
			1 Fox
31	NAVSEA		
	5 SEA 05R	3	CIT
	1 SEA 55		1 AERO Lib
	3 SEA 55N		1 Acosta
	1 SEA 55W		1 Wu
	3 SEA 56D		
	1 SEA 56X	4	U. Iowa
	3 SEA 56X1		1 Lib
	1 SEA 56X2		1 IHR/Kennedy
	3 SEA 56X7		1 IHR/Stern
	1 SEA 56X5		1 IHR/Patel

INITIAL DISTRIBUTION (Continued)

Copies		Copies	
3	U. Michigan/Dept Name	1	WHOI Ocean Engr Dept
	1 Name Lib		
	1 Parsons	1	WPI Alden Hydr Lab Lib
	1 Vorus		
		1	ASME/Res Comm Info
3	MIT		
	1 Barker Engr Lib	1	ASNE
	2 Ocean Engr/Kerwin		
		1	SNAME/Tech Lib
3	State U Maritime Coll		
	1 ARL Lib	1	AERO Jet-General/Beckwith
	1 Engr Dept		
	1 Inst Math Sci	1	Allis Chalmers, York, PA
4	Penn State U ARL	1	AVCO Lycoming
	1 Lib		
	1 Henderson	1	Baker Manufacturing
	1 Gearhart		
	1 Thompson	1	Bird-Johnson Co/Norton
1	Boeing Adv Amr Sys Div	1	Douglas Aircraft/Lib
1	BB&N/Jackson	2	Exxon Res Div
			1 Lib
1	Brewer Engr Lab		1 Fitzgerald
1	Cambridge Acous/Junger	1	Friede & Goldman/Michel
1	Calspan, Inc/Ritter	1	General Dynamics, EB/Boatwright
1	Stanford U/Ashley		
		1	Gibbs & Cox/Lib
1	Stanford Res Inst Lib		
		1	Rosenblatt & Son/Lib
2	Sit Davidson Lab		
	1 Lib	1	Grumman Aerospace/Carl
	1 Savitski		
		1	Tracor Hydronautics/Lib
1	Texas U ARL Lib		
		1	Ingalls Shipbuilding
1	Utah State U/Jeppson		
		1	Inst for Defense Anal
2	VPI/Dept Aero & Ocean Engr		
	1 Schetz	1	Itek Vidya
	1 Kaplan		
		1	Lips Duran/Kress
2	Webb Inst		
	1 Ward	1	Littleton R & Engr Corp/Reed
	1 Hadler		

28

Copies			CENTER DISTRIBUTION (Cont.)		
			Copies	Code	Name
1	Litton Industries				
1	Lockheed, Sunnyvale/Waid		1	152	Lin
2	McDonnel Douglas,		1	1521	Day
	Long Beach		1	1521	Karafiath
	1 Cebeci		1	1521	Hurwitz
	1 Hess				
			1	1522	Remmers
1	Maritech, Inc/Vassilopoulis		1	1522	Wilson
2	HRA, Inc		1	154	McCarthy
	1 Cox				
	1 Scherer		1	154.1	Yim
1	Nielsen Engr/Spangler		1	1542	Huang
1	NKF Associates/Noonan		35	1544	Chen
			1	1544	Kim
1	NAR Space/Ujihara		1	1544	Reed
2	Atlantic Applied Research		1	156	Cieslowski
	1 Brown				
	1 Greeley		1	172	Krenzke
1	Propulsion Dynamics, Inc		1	1720.6	Rockwell
1	Sperry Sys Mgmt Lib/Shapiro		1	19	Sevik
1	OF Technologies/Furuya		1	1901	Strasberg
1	UA Hamilton Standard/		1	1905	Blake
	Cornell				
			1	1906	Biancardi
	CENTER DISTRIBUTION		1	1942	Mathews
			1	1962	Kilcullen
Copies	Code	Name			
			10	522.4	Reports Control
1	0120				
			1	522.1	TIC (C)
1	12				
			1	522.2	TIC (A)
1	112.1	Nakonechny			
1	15	W.B. Morgan			
1	1506	Walden			
1	1508	Boswell			